Divalent Calcium Cation-Catalyzed Hydrolysis of Phosphodiester Bonds in Cyclic Dinucleotide Molecules

Arline Tarazona

Abstract

The main role of the secondary messenger that is found in *Vibrio cholerae* bacteria, 3', 3'-cyclic guanosine adenosine monophosphate (3', 3'-cGAMP), is to promote intestinal colonization of the bacteria by downregulating chemotaxis through an amplified internal signal. The cyclic molecule includes two phosphodiester bonds, known to have kinetically slow cleavage rates, and therefore, allow these molecules to be relatively stable. Phosphodiester bonds typically contain two negatively charged oxygen atoms, which are in resonance with each other, that repels incoming nucleophiles that try to attack the phosphorus atom. In order to increase the rate at which 3', 3'-cGAMP hydrolyzes and, consequently, terminate the signaling pathway, enzymes, such as some EAL-domain or HD-GYP-domain phosphodiesterases, utilize metal-ion cofactors to serve as catalysts. Metal-ion catalysts increase the electrophilicity of the phosphorus and, consequently, increase the rate of hydrolysis of the secondary messenger. In enzyme active-sites, metal-ions can also activate the nucleophile for attack on the phosphorus; however, the mechanism by which metal-ion-catalyzed phosphodiester cleavage of 3', 3'-cGAMP occurs under aqueous conditions is not known. After performing kinetic trials, reverse-phase high performance liquid chromatography (HPLC) can monitor changes in substrate and reactant concentrations, which were plotted as a function of time to produce rate constants. The chromatographs obtained from HPLC are believed to reveal the generation of four products, 2'-AMP, 3'-AMP, 2'-GMP and 3'-GMP, with no accumulation of intermediates, which suggests that the initial cleavage of 3', 3'-cGAMP is rate-limiting. The metal-ion-assisted hydrolysis of 3', 3'-cGAMP is validated by the breakdown of the reactant and formation of products. Plotting rate constants as a function of Ca^{2+} concentrations yielded a saturating rate constant value of $1.3x10^{-2}$ min^{-1} and a rate constant value, at 0 M Ca^{2+}, of $6.8x10^{-5}$ min^{-1}, which show a catalytic

effect of 190-fold, and an equilibrium dissociation constant value of 0.48. The secondary plot shows a rectangular hyperbola trend that is consistent with a saturating single-metal-ion mechanism, which is also observed with RNA. Uncovering the mechanism by which 3', 3'-cGAMP hydrolyzes can help determine whether this cleavage is consistent with the observed RNA cleavage by the activated 2'-OH group. A second model system, 2', 3'-cyclic guanosine adenosine monophosphate (2', 3'-cGAMP) is used to compare its products formed to the products formed of 3', 3'-cGAMP in Ca^{2+} solution. Comparing between the 3', 3'-cGAMP and 2', 3'-cGAMP reactions can reveal how slight changes in phosphate linkages can impact the 2'OH- induced intramolecular attack on the electrophilic phosphorus. One of the effects as a result of the changes in phosphate linkages, for instance, can be seen in the catalytic defect of about 30-times in the rate constant for the hydrolysis reaction, when the substrate is changed from 2', 3'-cGAMP to 3', 3'-cGAMP.

Contents

Section A: Introduction

I. Biological Significance of Phosphodiester Bonds and Cyclic-di-NMPs

Phosphodiester bonds can be found in many molecules of biological importance, such as deoxyribonucleic acids, ribonucleic acids, and many signaling molecules (Robinson et al, 1995; Smith et al, 2012). Phosphodiester bonds contain two negatively-charged oxygen atoms, which are in resonance with each other, that repel incoming nucleophiles that try to attack the phosphorus atom (Westheimer, 1987). The negatively-charged nature of the phosphodiester bonds proves to be a challenge when these phosphodiester bonds need to be hydrolyzed, or broken down. While hydrolysis of phosphodiester bonds is kinetically unfavorable, the hydrolysis is known to be thermodynamically favorable, which suggests that enzymes or catalysts can increase the rate by which phosphodiester bonds hydrolyze (Cassano et al, 2004). Phosphodiester bonds, therefore, provide kinetic stabilization of these molecules in biological systems (Král et al, 2006). Kinetic stabilization of these biological molecules, specifically RNA and DNA, are absolutely necessary and crucial to sustain life on earth, because they are the molecules that hold together genetic information and are the precursors to proteins in protein synthesis. Through transcription, a DNA molecule acts as the template for the synthesis of an RNA molecule. In translation, the RNA encodes for the amino acid sequences to generate a full-length protein. Proteins perform a variety of functions that ultimately support the existence of life. Other biological molecules, including as signaling molecules, also support the lives of living organisms by allowing the transmission of important information. Many of these signaling molecules also contain phosphodiester bonds that help with the stability of the molecules.

In prokaryotes and eukaryotes, nucleotide molecules, specifically signaling molecules, are necessary for the regulation of certain cellular reactions that are characteristic of the organisms and for their basic survival. The signaling molecule, cyclic-adenosine-monophosphate (cAMP), is found in eukaryotic organisms and is responsible for modulating certain proteins, specifically kinases and ion channels, that regulate cellular processes, such as vision maintenance, electrolyte homeostasis and smooth muscle relaxation (Kalia et al, 2013). Cyclic-guanosine-monophosphate (cGMP), is another signaling molecule that can be found in bacteria, which is thought to be involved in quorum sensing, where genes are regulated according to changes in bacterial population density (Kalia et al, 2013). Bacterial di-nucleotide signaling molecule, cyclic-di-AMP, is responsible for cell wall homeostasis in response to external stressors (Kalia et al, 2013). Another cyclic di-nucleotide signaling molecule, such as cyclic-di-GMP, is responsible for biofilm formation and for the production of virulence factors in certain bacteria (Kalia et al, 2013). All of these different signaling molecules prove to be essential for the basic functioning of either eukaryotic or prokaryotic organisms.

Two specific signaling molecules of interest are 3', 3'-cyclic-guanosine-adenosine monophosphate (3', 3'-cGAMP) and 2', 3'-cyclic-guanosine-adenosine-monophosphate (2',3'-cGAMP). 2', 3'-cGAMP contains a 2'-5' and a 3'-5' linkage, while 3', 3'-cGAMP contains two 3'-5' phosphate linkages (see Figure 1). Both molecules are di-cyclic molecules that contain a guanosine and an adenosine nucleotide base (see Figure 1).

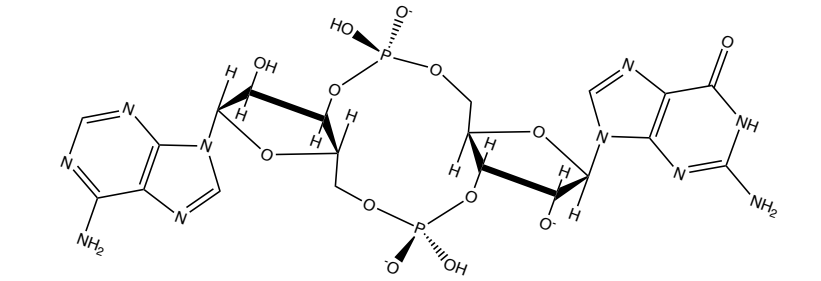

a)

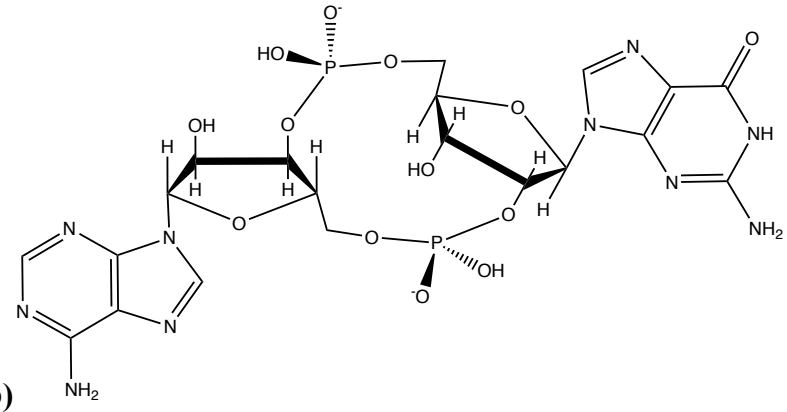

b)

Figure 1: Molecular structures of di-nucleotide secondary messengers. Figure 1a represents the molecular structure of 3', 3'-cGAMP, which is the secondary messenger found in prokaryotes. Figure 1b represents the molecular structure of 2', 3'-cGAMP, which is a eukaryotic secondary messenger.

3', 3'-cGAMP is a secondary messenger found in *Vibrio cholerae* that helps with its colonization in human intestines (Gao et al, 2015). 3', 3'-cGAMP will downregulate chemotaxis and relay the internalized and amplified signal and induce intestinal colonization (Hallberg et al, 2016). Moreover, in order for *V. cholerae* bacteria to survive and thrive in the human intestines once the bacteria are ingested, typically through contaminated drinking water, the bacteria will need to settle in the intestines and start multiplying. The dinucleotide cyclase that synthesizes 3', 3'-cGAMP is DncV. Because the signaling molecule's pathway is considered ancient, however, other research studies suggest that more than one dinucleotide cyclase exists that synthesize 3',

3’-cGAMP (Gao et al, 2015). Other signaling molecules are capable of playing a similar role as 3’, 3’-cGAMP.

Another signaling molecule that plays a role in the survival of living organisms – this time in eukaryotic organisms – is 2’, 3’-cyclic-guanosine-adenosine monophosphate (2’,3’-cGAMP). The dinucleotide cyclase that synthesizes 2’, 3’-cGAMP is cGAS (Kranzusch et al, 2014). 2’, 3’-cGAMP is specifically responsible for promoting innate immunity by the inducing Type-I interferons, in response to an invasion of foreign DNA material (Wu et al, 2013). When activated, both di-nucleotide signaling molecules contribute to the survival of living organisms. When these signaling molecules are no longer needed for their function, they must be hydrolyzed; not much is known about the hydrolytic mechanisms of 3’, 3’-cGAMP and 2’, 3’-cGAMP.

When the signaling molecules no longer need to be activated, and the cells no longer require the chemical messages produced by these secondary messengers, the signaling pathway that produces the relay of these chemical messages will have to be terminated. In order to stop the signaling pathway, the phosphodiester bonds of the signaling molecule will need to be hydrolyzed, or degraded. Each of these signaling molecules have different chemical and structural features (see Figure 1). For instance, signaling molecules can have either a cyclic or linear nature, they can be made of either one or nucleotide bases, or their phosphate linkages may vary. Both 3’, 3’-cGAMP and 2’, 3’-cGAMP have two different nucleotide bases, guanosine and adenosine bases, and have a cyclic nature. The structural difference between both of them is the orientation of their phosphate linkages. Their chemical properties vary depending on their individual role in a specific type of organism and in an enzyme active-site. Therefore, the mechanism by which these molecules hydrolyze may vary depending on their molecular

structure (Kalia et al, 2013). Furthermore, the half-life of many signaling molecules in the absence of the enzymes that hydrolyze them can be as high as several hundred to thousands of years.

II. Enzymes and Mechanisms of Catalysis Related to Phosphodiesterases

To potentially decrease the half-lives of these cyclic-di-nucleotide monophosphates (c-di-NMPs), enzymes need to be introduced into the system. Enzymes are proteins that help reactions occur at a faster rate, by lowering the activation energy barrier of the reaction. Enzymes that specifically break down phosphodiester bonds are known as phosphodiesterases. In order to understand how the phosphodiester bonds of the existing signaling molecules break down, their hydrolysis mechanisms can be compared to the more established hydrolysis mechanisms of DNA and RNA models.

The mechanism by which a phosphodiester bond cleaves involves a phosphoryl-transfer reaction. A phosphoryl transfer reaction is defined as the transfer of a phosphoryl group (PO_3^-) from a phosphate ester or anhydride to a nucleophile (Hengge, 2015). Because phosphoryl-transfer reactions naturally have very slow rates, they typically need the assistance of enzymes to speed up the rate of the reaction and to decrease the kinetic energy barrier (Hengge, 2015). When a phosphoryl group is transferred from the leaving group to the nucleophile, changes in electrostatic or geometric conditions may occur, as the reaction moves from the ground state to the transition state (Lassila et al, 2011). Some models propose that during a phosphoryl-transfer reaction, metal-ion cofactors of a biological enzyme in an enzyme active-site, interact with the two non-bridging oxygen atoms on the transferred phosphoryl group to neutralize the negative charge in the transition state (Lassila et al, 2011). As the reaction proceeds to the transition state, geometric changes can also occur. Without the assistance of an enzyme, the solvent in the

reaction would have to rearrange to be able to accommodate the transition states (Lassila et al, 2011). However, with the assistance of an enzyme, the enzyme folds and accommodates and interacts with the transition state (Lassila et al, 2011). These transition states that form in a catalyzed reaction allow for a lower energy barrier than in an un-catalyzed reaction.

Both DNA and RNA molecules contain phosphodiester bonds, which can be broken down by be enzymes that utilize metal-ions. RNA contains a 2'-hydroxyl group, which DNA lacks, that is in close proximity to the electrophilic phosphorus and can be deprotonated in basic solution; the deprotonated 2'-hydroxyl group can act as nucleophile that attacks the phosphorus intramolecularly (Li et al, 1999). The metal-ion can be either directly bound to the 2'-hydroxyl group, which is considered inner-sphere coordination, or indirectly bound to the 2'-hyrdoxyl group, which is considered outer-sphere coordination (Chval et al, 2011). While this scheme is observed in ribozyme models (Chval et al, 2011), it can also be observed in aqueous models (Kirk et al, 2010). The mechanism by which RNA hydrolyzes is mononuclear, in which a single metal-ion is involved in the hydrolysis of the phosphodiester bonds (Messina, 2014). One of the main characteristics that differentiates between phosphodiester models is the number of metal-ions that are used in their hydrolysis mechanisms.

III. Role of Metal-Ions in Phosphodiester Hydrolysis Reactions

DNA models are types of phosphodiester models that lack an internal nucleophile, so the mechanism by which they hydrolyze is known to be different because of this structural characteristic. The mechanism by which DNA models hydrolyze is di-nuclear for Ca^{2+}, which means that two metal-ions are involved in the hydrolysis of the phosphodiester bonds found in DNA (Kirk et al, 2010). The chemical structure that was discussed previously may contribute to the difference in mechanism, because the metal-ions would have to coordinate with two non-

bridging oxygen atoms while coordinating with an external hydroxide ion nucleophile (Kirk et al, 2010). In a DNA model that exhibits a di-nuclear mechanism, the two metal-ions may have to position a hydroxide-ion for attack on the phosphorus (Kirk et al, 2010). RNA and DNA and metal-ion model systems can be compared to certain cyclic di-nucleotide models.

Metal-ions fulfill multiple roles in enzyme active-sites. In general-base catalysis, the metal-ion can form a complex with a hydroxide-ion, which can then coordinate with one of the non-bridging oxygen atoms on the phosphorus and also induce an intramolecular attack on the phosphorus by removing the hydrogen atom on the 2'-OH group, which can be found in RNA models (Korhonen et al, 2013). In general-acid catalysis the metal-ion can form a complex with a water molecule and stabilize the leaving group by coordinating with one of the negatively-charged non-bridging oxygen atoms of the phosphorane intermediate (Mikkola et al, 1999). They can be utilized in various catalytic strategies, such as metal-ion and general acid-base reactions (Bruice et al, 1996) (see Scheme 1 below).

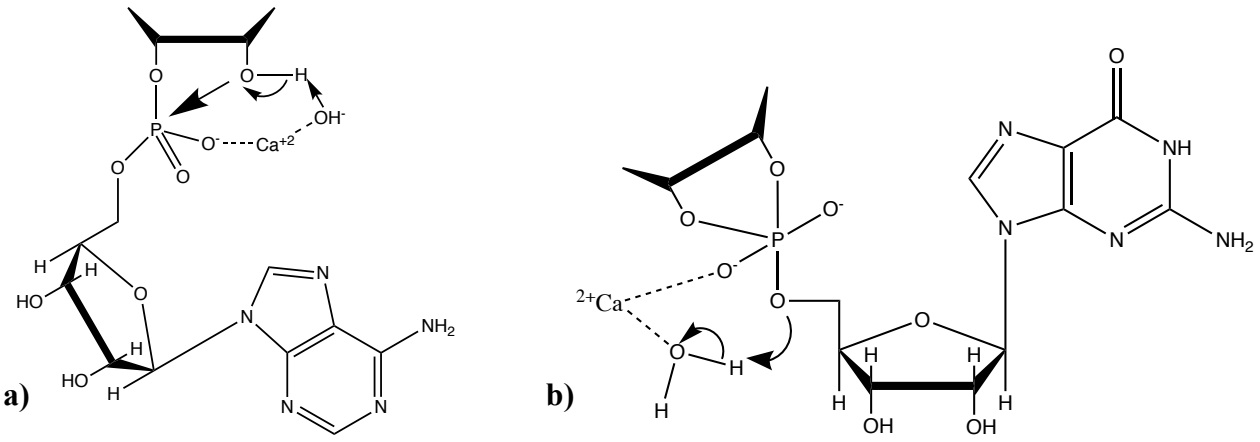

Scheme 1: General schemes of acid-base metal-ion-based catalysis in RNA models. Scheme 1a represents a general-base metal-ion-based catalytic mechanism. In Scheme 1a, the Ca^{2+} ion coordinates with a hydroxide ion and positions it so that it can remove the hydrogen atom away from the 2'-OH group, or acts as a base by accepting the hydrogen from the 2'-OH group. The 2'-OH group becomes negatively charged oxygen atom, which is the internal nucleophile that attacks the phosphate intramolecularly. Scheme 1b represents a general-acid metal-ion-based catalytic mechanism. In Scheme 1b, a Ca^{2+} ion coordinates with a water molecule and positions

it so that the H_2O molecule can donate a proton to the 5'-linked oxygen from the phosphorane intermediate, which then, as result, becomes a stabilized leaving group.

Hydrolytic reactions of phosphodiester bonds can be facilitated by general acid-base reactions. Both general acid-catalyzed and base-catalyzed reactions proceed through an S_N2 mechanism (Li and Breaker, 1999). In the S_N2 hydrolytic reaction of the phosphodiester bond of an RNA molecule, the 2'-oxyanion attacks the nearby phosphorus atom, which is known as a specific base-catalyzed rection (Li and Breaker, 1999). The protonation state of the 2'-oxygen group is what determines the rate of cleavage of the phosphodiester bonds that connect the nucleotides together in the molecule (Li and Breaker, 1999).

Not only does the protonation state of the 2'-oxygen group determine the rate of cleavage, but the higher-ordered structures of RNA molecules, such as those structures of RNA molecules with hairpin loops, also determine the rate of phosphodiester cleavage (Li and Breaker, 1999). The structure of the RNA molecules can influence the transesterification and hydrolysis reactions of phosphodiester molecules. For instance, the hydrolysis reaction of duplex RNA, which is less flexible than single-stranded RNA, is inhibited due the duplex structure of the RNA (Hegg et al, 1997). This inhibition is due to the decreased flexibility, where the 2'-hydroxyl group must orient itself to become adjacent to the phosphorus center and then perform an in-line displacement upon attack on the phosphorus (Hegg et al, 1997). This decreased flexibility found in RNA molecules can also be found in cyclic-di-NMPs, which can also explain their constrained nature. Enzymes, such as phosphodiesterases, eventually have to fit the entire molecule within its active-site, and modify certain features within its active-site in order to be able to hydrolyze the phosphodiester bonds.

Biological enzymes must be able to position the nucleophile, which under alkaline conditions, is the deprotonated 2'-hydroxyl group, so that it is aligned with the phosphorus atom and leaving

group for an in-line attack on the phosphorus (Lassila et al, 2011). Enzymes, especially those with metal-ion cofactors, serve other roles in an enzyme-active site so that catalysis can occur. Because of the negative charge on the phosphodiesters, positively-charged metal-ion cofactors can interact with that negative charge during catalysis (Bruice et al, 1996). The enzymes that break down cyclic-dinucleotides, including 3',3'-cGAMP and cyclic-di-GMP, belong to the EAL protein domain, which are known to utilize two metal-ions that assist in phosphodiester cleavage (see Scheme 2 below) (Tchigvintsev et al, 2010). Phosphodiesterases that belong to the EAL domain are known to require divalent metal ions, such as Mg^{2+} and Mn^{2+}, where the most efficient catalytic activity occurs under alkaline conditions, specifically conditions where the pH is greater than 7 (Bellini et al, 2017). While not much research has been done on the mechanism of the catalytic hydrolysis of 3', 3'-cGAMP, research has been done on the hydrolytic reaction mechanisms of other cyclic di-nucleotides, such as cyclic-di-GMP.

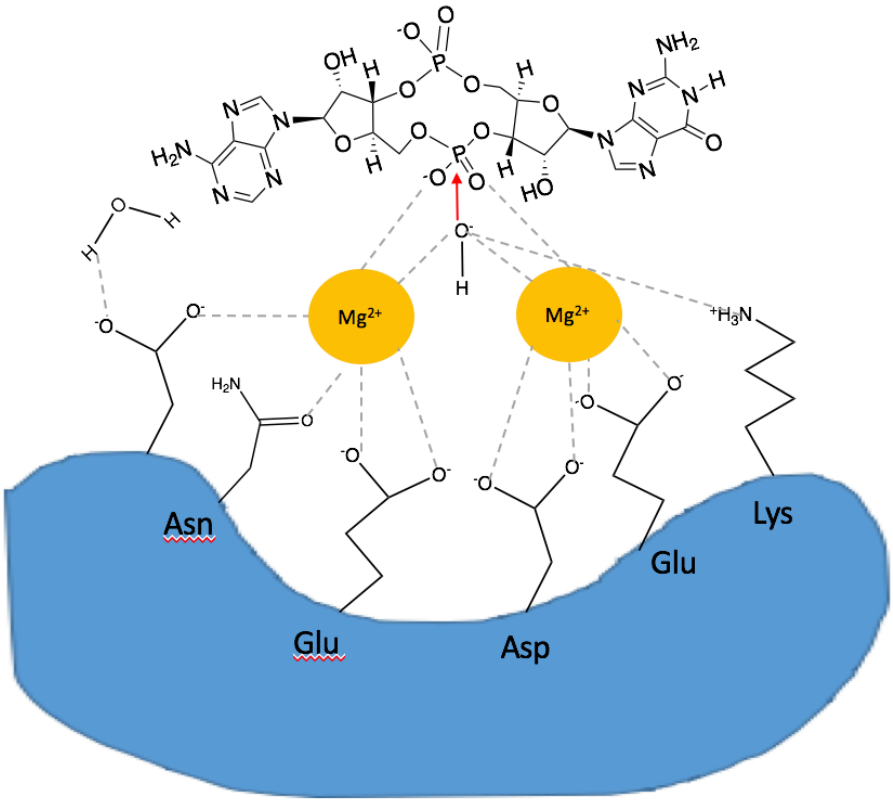

(Adapted from Tchigvintsev et al, 2010)

Scheme 2: Enzyme active-site belonging to EAL domain of phosphodiesterases. This figure represents a hydrolysis reaction of 3', 3'-cGAMP, where the enzyme (represented in blue) and its amino acid residues are coordinating with two Mg^{2+} ion. The two metal-ions, in turn, are coordinating with a hydroxyl group that acts as a nucleophile that attacks the phosphorus center of the 3', 3'-cGAMP substrate.

Cyclic-di-GMP is also a secondary messenger found in bacteria, and it has a chemical structure that is homologous to the structure of 3', 3'-cGAMP, with the only structural difference being that one of the nucleotide bases on cyclic-di-GMP is a guanosine rather than an adenosine (Bellini et al, 2017). The homologous structures between cyclic-di-GMP and 3', 3'-cGAMP suggest that they should be able to react and hydrolyze in a similar manner. The EAL-domain phosphodiesterases are generally known to contain two metal-ions that coordinate with a water molecule, which may act as a nucleophile in the hydrolytic reaction of the cyclic dinucleotide

(Shanahan et al, 2013). EAL-domain phosphodiesterases catalyze the cleavage of phosphodiester bonds of cyclic-di-GMP by cleaving one of the phosphoester bonds to then give a linear dinucleotide 5'-pGpG (see Scheme 3 below) (Minasov et al, 2009). The linear dinucleotide is then further cleaved to the GMP products (see Scheme 3 below) (Schmidt et al, 2005). Because they are both similar in terms of their molecular structures, their enzyme-active sites should also be similar. In other words, both of their enzyme active-sites should contain similar features that aid catalysis.

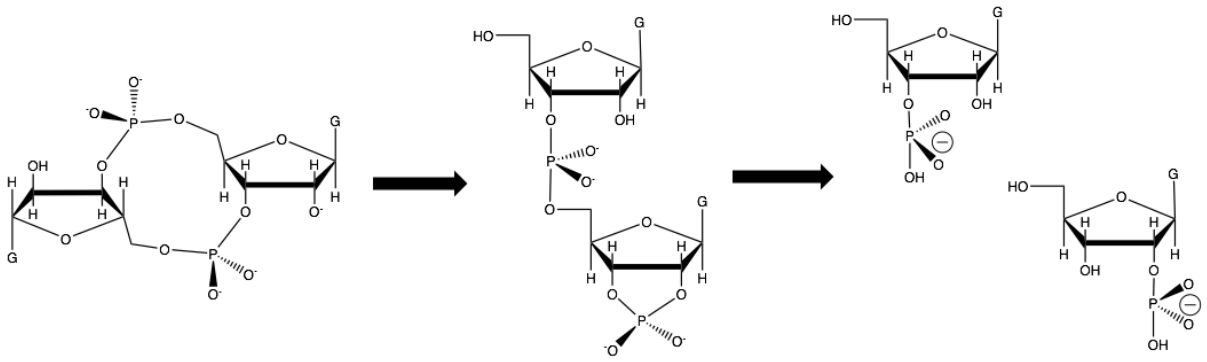

(Adapted from Rao et al, 2008)

Scheme 3: Overall hydrolysis mechanism for secondary messenger, cyclic-di-GMP. After the cleavage of one of the phosphoester bonds, a linearized dinucleotide intermediate, 5'-GpGcp forms. The final cleavage of the remaining phosphoester bonds leads to the formation of the GMP products, 2'GMP and 3'-GMP.

Certain features found within active-sites of EAL-domain proteins aid the enzyme-catalyzed hydrolysis of biological molecules. For instance, coordination and non-covalent interactions between the protein residues, metal-ions, hydroxide ions and water molecules contribute to the stabilization of the active site and contribute to the catalysis of the hydrolytic reactions of the secondary messenger molecules (Bellini et al, 2014). Within the enzyme active-site of EAL domain phosphodiesterases, two metal-ions are each suggested to be in contact with a different non-bridging oxygen atom that is bonded to the phosphorus atom (Shanahan et al, 2013).

Various metal-ions can be used to form interactions and coordinations with the non-bridging oxygen atoms found in phosphodiester models.

A lot of studies involving the hydrolysis of phosphodiester bonds usually involve the use of divalent metal-ions. Divalent metal ions, such as Mg^{2+}, Mn^{2+} and Zn^{2+}, are good catalysts that are useful in the hydrolysis of phosphodiester bonds (Zhan and Zheng, 2001). The water molecules can coordinate with the metal ions and can act as general bases once they become deprotonated, typically by protein residues (Rao et al, 2008). The interactions between the metal ion(s) and non-bridging oxygen atoms on the molecule will pull electron density away from the phosphate and, consequently, make the phosphorus electrophilic and vulnerable to attack from an external nucleophile (Bruice et al, 1996). Metal-ions can act as Lewis-acids and neutralize the negative charges on the non-bridging oxygen atoms, thus leading to an increased susceptibility to nucleophilic attack (Verma et al, 2009). In enzyme-active sites, multiple metal-ions may be necessary to fulfill the roles involved in the hydrolysis of a molecule's phosphodiester bonds.

Various mechanisms of metal-ion catalysis include: lowering the pKa of coordinated water molecules in order to increase the hydroxide-ion concentration in solution, stabilizing the transition state by interacting with the phosphomonoester and nucleophile, and stabilizing the negatively-charged leaving group (Cassano et al, 2004). Metal-ion catalysis is made possible by the favorable interactions between the structural elements found in enzyme active-sites and the non-bridging oxygen atoms on the phosphodiester bonds. Some examples of phosphodiesterases, such as the hammerhead ribozyme and the NPP1 enzyme, use metal-ions to aid in the catalytic hydrolysis of their phosphodiester substrates. The enzyme, Ecto-nucleotide pyrophosphatase phosphodiesterase 1 (ENPP1), which is also known as the NPP1 enzyme, is known to specifically bind to and degrade 2', 3'-cGAMP – but not 3', 3'-cGAMP (Kato et al, 2018).

According to Scheme 2, an enzyme active-site can be thought of as a stable complex that consists of numerous interactions between the amino acid residues and the components of the enzyme active-site. Other components of the active-site, besides the amino acid residues, typically include water molecules and metal ions. EAL-domain phosphodiesterases are typically known to utilize two metal-ions, such as magnesium metal ions (Shanahan et al, 2013). Depending on the pH conditions of the active-site, hydroxyl ions may naturally exist in the solution, which can act as the nucleophile and cause the hydrolysis of the phosphodiester bonds of the substrate.

Many phosphodiesterases are known to use metal-ions to assist in phosphodiester cleavage. Similar to the EAL-domain phosphodiesterases, the hammerhead ribozyme is known to use two metal ions to catalyze the cleavage of RNA molecules. While the RNA hydrolysis is known to require the assistance of a single metal-ion, the hammerhead ribozyme exists as an alternative RNA-phosphodiesterase that uses two-metal ions. According to the mechanism of the ribozyme, the first metal ion deprotonates the 2'-OH group, and the second metal-ion facilitates the departure of the leaving group (Bruice et al, 1996). The 2', 3'-cGAMP molecule is also known to be hydrolyzed by a two-metal-ion mechanism.

The hydrolysis of 2', 3'-cGAMP, by the nucleotide pyrophosphate/ phosphodiesterase 1 (NPP1) enzyme active-site, is known to produce 5'-AMP and 5'-GMP and typically utilizes two Zn^{2+} metal-ions as cofactors that aid in the catalytic hydrolysis of the molecule's phosphodiester bonds (Namasivayam et al, 2017). However, the 5'-AMP and 5'-GMP may not necessarily be the same products observed with the aqueous model system studies. While the enzyme active-site of NPP1 may contain structural and catalytic features that can contribute to the hydrolytic mechanism that is observed, comparing the kinetic results between aqueous model systems and

enzyme active-sites would be interesting to note. NPP1 functions optimally under alkaline conditions and, thus, the mechanism by 2', 3'-cGAMP hydrolyzes in the enzyme active-site can have similar results to the way 2', 3'-cGAMP hydrolyzes in an aqueous model system that is also under alkaline pH conditions. One observation that was noted when the NPP1 assisted in the hydrolysis of 2', 3'-cGAMP was that the hydrolytic steps leading to the break-down of intermediates occurred very quickly that no linear intermediate products were seen – only the final products, 5'-AMP and 5'-GMP were seen (Namasivayam et al, 2017). Comparing the intermediates and products formed between enzyme active-site models and aqueous models can elucidate information on the effects certain active-site features have on the hydrolysis mechanism of the phosphodiester molecules, specifically of the 2', 3'-cGAMP and 3', 3'-cGAMP molecules. Both of these molecules are interesting to study under the conditions of an enzyme active site because of their slight differences in phosphodiester linkages.

Enzymes bind to their specific substrate, as they have binding pockets specifically designed for certain substrates. Phosphodiesterases, which can belong to either the GGDEF, EAL or HD-GYP domain, are known to have slight amino acid sequence differences in their enzyme active-sites so that only certain cyclic dinucleotide molecules can bind and interact with the amino acid residues within the active-sites (Römling et al, 2017). Not only does the pH and metal-ion have an effect on the phosphodiester hydrolysis mechanism, but the enzyme active-site itself can have its effects. Considering enzyme active-sites contain varying amounts and types of metal-ion cofactors, different interactions between the metal-ion cofactors and the substrate are expected. Moreover, different mechanisms can be observed according to the type or class of phosphodiesterases. According to different phosphodiester models, phosphodiester hydrolysis can occur either through a concerted or through a stepwise mechanism (Cassano et al, 2004). In a

concerted mechanism, the bond attached to the leaving group breaks while a bond to the nucleophile forms (Cassano et al, 2004). In a stepwise mechanism, a phosphorane intermediate is formed (Cassano et al, 2004). Whether one mechanism is seen versus the other often depends on the structure of the enzyme active-site and the types of interactions between other molecules or residues that are found within active-sites (Cassano et al, 2004). Interactions between the metal-ion(s) and the substrate ultimately correspond to the type of mechanism that is observed during phosphodiester hydrolysis.

IV. Aqueous Studies Using RNA Model Systems

Kinetic studies, that utilize aqueous model systems, have been done to examine the rate constants for the hydrolytic reactions of many phosphodiester models. Aqueous model systems allow for the close observation and examination of phosphodiester hydrolytic reaction mechanisms and schemes. Various types of aqueous models exist depending on the pH conditions of the system. The pH is an important factor to consider when utilizing an aqueous model system, because the pH conditions of the system can have an effect on the rate of cleavage of phosphodiester bonds. For instance, for RNA models, under neutral and acidic conditions pseudorotation around the phosphorus atom can occur and form isomers of the starting material (Mikkola et al, 1999). Under alkaline conditions, however, the phosphorane intermediate is very short-lived, so psuedorotation and isomerization should not occur, and only cleavage of the phosphodiester bond should be observed (Korhonen et al, 2013). Therefore, under alkaline conditions, depending on the leaving group, the hydroxide-catalyzed hydrolysis of the phosphodiester bond can involve a concerted mechanism (Cassano et al, 2004). In a typical hydro\lytic reaction of an RNA molecule at alkaline conditions, a deprotonated 2'-OH acts as a nucleophile and attacks the electrophilic phosphorus atom (Oivanen et al, 1998).

Studies done on the hydrolysis of RNA molecules can be used as foundation for studies that are being done on the hydrolysis of cyclic di-nucleotide molecules. Kinetic studies under aqueous conditions have already been done on the hydrolysis of 2', 3'-cyclic-di-AMP (see Scheme 5 below). The hydrolysis mechanism of RNA molecules should be similar to the hydrolysis mechanism of cyclic di-nucleotide secondary messengers, so long as the molecules have a 2'-OH that can induce an intramolecular attack on the phosphorus found in the phosphodiester linkage. The reaction scheme for RNA hydrolysis, and also for the hydrolysis of some cyclic secondary messengers, under aqueous alkaline conditions, initially involves the intramolecular displacement of the 5'-linked nucleoside by the 2'-oxyanion, or the 2'-OH group that became deprotonated in aqueous solution (Scheme 6) (Oivanen et al, 1998). This intramolecular displacement is a likely step that occurs under alkaline conditions, because the initial 3',5'-phosphodiester bonds in the intermediate do not isomerize to 2',5'- phosphodiester bonds that could occur concurrently with hydrolysis (Oivanen et al, 1991). The intermediates that are formed are 2', 3'-cyclic phosphates, which typically hydrolyze quickly to a combination of 2'- and 3'-phosphate products (Oivanen et al, 1998). Despite the fast hydrolysis of the 2', 3'-cyclic phosphate intermediates, these intermediates can still be detected (Oivanen et al, 1998). Understanding how fast these intermediates disappear in a reaction can elucidate information on the type of mechanism by which the phosphodiester models hydrolyze.

The mechanism by which RNA models hydrolyze can depend on their type of secondary structure. For instance, the hydrolysis of an RNA molecule with a loop secondary structure is not as efficient as that of a linear RNA molecule, when the catalytic hydrolysis is mediated by a metal-ion (Zagórowska et al, 1998). However, one study concluded that when the zinc metal-ion is introduced into the system, the hydrolysis of the phosphodiester bonds in a loop-structured

RNA molecule becomes similar to the hydrolysis of the phosphodiester bonds in a linear RNA molecule (Zagórowska et al, 1998). The zinc metal-ion appears to be efficient at significantly increasing the rate of hydrolysis of the RNA molecule. The study also demonstrated that the zinc metal-ion coordinates with both phosphate groups, which is seen in studies on the hydrolysis of RNA models (Zagórowska et al, 1998). Moreover, these observations further prove that the metal-ion-assisted hydrolysis of RNA molecules is influenced by the choice of metal-ion and by the structure of substrate. For instance, when 5-uridine-guanosine 3' (UpG), or an RNA model, is subjected to basic pH conditions, its 2'-OH group can be deprotonated and eventually attack the electrophilic phosphorus center that is in close proximity to it (see Scheme 4 below). When working under alkaline and under aqueous model conditions, including metal-ions that are particularly soluble at high pH conditions, such as Ca^{2+}, will assist in the coordination of the non-bridging negatively-charged oxygen atoms (see Scheme 4 below).

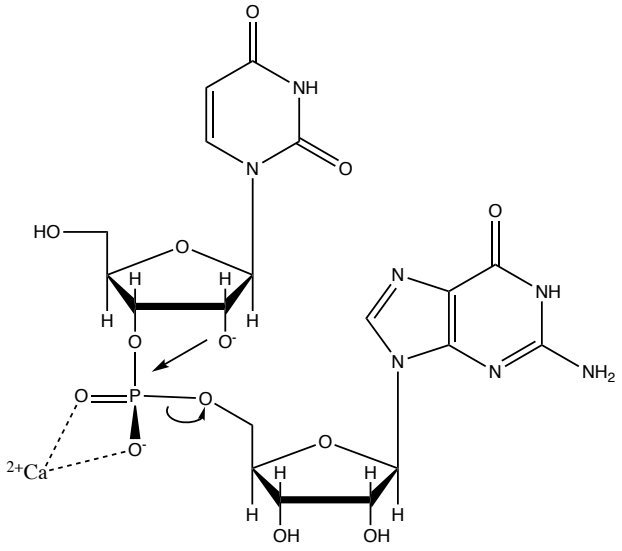

Scheme 4: General scheme of the divalent calcium metal-ion-assisted cleavage of UpG phosphodiester bond. The cleavage is initiated by the internal nucleophile, which can become activated under basic conditions in an aqueous model system.

This project will explore how metal-ion catalysts can possibly have an effect, such as a significant increase, on the rate of hydrolysis of the possible intermediates. Some research has

already been done regarding the enzymes that break down our molecule of interest, 3', 3'-cGAMP. Important features of these enzyme active-sites include metal-ion cofactors, which are found within enzyme active-sites, are known to aid in catalytic and hydrolytic activity of the phosphodiesterases.

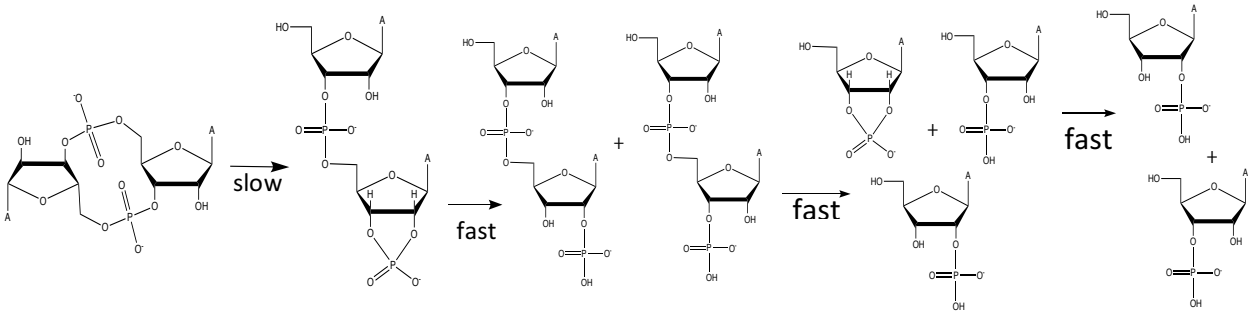

(Mechanism scheme adapted from Ora et al, 2013)

Scheme 5: Mechanism of the hydrolytic reaction of cyclic-di-AMP, under alkaline conditions. After the deprotonated 2'-OH internal nucleophile attacks the phosphorus, a 2', 3'-cyclic phosphate linkage is formed. Afterward, either the 2'-hydroxy or 3'-hydroxy group is displaced by a hydroxide-ion nucleophile. Further cleavage of the other phosphodiester bond yields a mixture of 2'-AMP and 3'-AMP products (Ora et al, 2013).

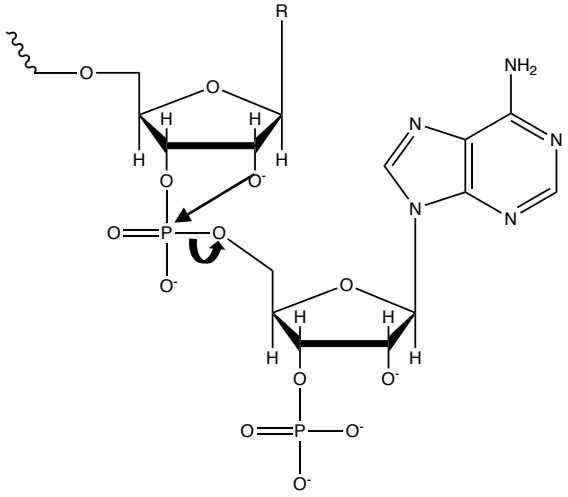

Scheme 6: General scheme of intermolecular attack on phosphorus. The RNA model has a deprotonated 2'-OH group that attacks the phosphorus, which eventually leads to the departure of the leaving group.

In order to simply look specifically at the cleavage of phosphodiester models and not produce any other products as a result of side reactions due to acidic or neutral pH conditions,

phosphodiester cleavage under alkaline conditions are often studied. Under alkaline conditions, alkaline earth metal ions, such as Mg^{2+} and Ca^{2+} are often used, because they efficiently induce phosphodiester cleavage (Yashiro et al, 2002). Other alkaline earth metal ions, such as Sr^{2+} and Ba^{2+} can also induce phosphodiester cleavage however, not as efficiently as Mg^{2+} and Ca^{2+} (Yashiro et al, 2002). Meanwhile, Na^{+} and K^{+} were determined to have a very low effect on phosphodiester cleavage (Yashiro et al, 2002). The type of metal-ion used in kinetic studies that observe phosphodiester hydrolysis rates is crucial, because the metal-ion, along with the pH conditions of the system, have effects on the type of catalytic mechanism that occurs between the metal-ion and the phosphodiester substrate.

V. Kinetic Studies on Hydrolytic Reaction of 3', 3'-cGAMP

After phosphodiester hydrolysis of 3', 3'-cGAMP, four products are expected to be seen: 2'-AMP, 2'-GMP, 3'-AMP, 3'-GMP. The cyclic-dinucleotide, c-di-AMP, which is structurally homologous to 3', 3'-cGAMP, is also known to cleave at a slower rate than RNA, and is, therefore, more stable than RNA (Ora et al, 2013). Moreover, 3', 3'-cGAMP is suspected to also cleave at a slower rate than RNA. Phosphoester bonds are very resistant to hydrolysis, which is proven by the extremely long half-lives of DNA and RNA (Komiyama and Sumaoka, 1998). For instance, the half-life of the phosphodiester bond in DNA at pH 7 and 25ºC is about 200 million years, and the half-life of the phosphodiester bond in RNA, also at pH 7 and 25ºC, is about 1,000 years (Komiyama and Sumaoka, 1998). Even in an enzyme active-site, such as the Hammerhead ribozyme, without using any metal-ions to assist with the cleavage of the phosphodiester linkage, the half-life of the RNA backbone is approximately 110 years at pH 7 and 25°C (Torres et al, 2003). The breaking of these phosphodiester bonds, therefore, require the assistance of an

enzyme to help lower the energy barrier to achieve the hydrolyzed 3', 3'-cGAMP molecule at a significantly fast rate.

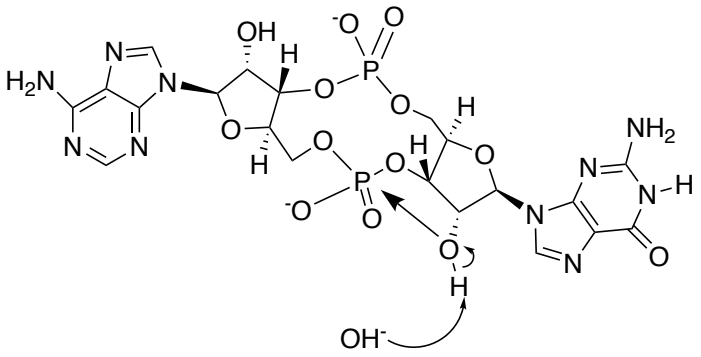

Scheme 7: The hydrolysis reaction of 3', 3'-cGAMP under alkaline conditions. Hydroxide ions found in solution can deprotonate the 2'-OH group. The 2'-alkoxide ion can then act as a nucleophile and attack the phosphorus center.

Research studies on the hydrolysis of other phosphodiester models, such as cyclic-di-AMP, can used as a way to compare any similarities between the mechanisms of cyclic-di-AMP and 3', 3'-cGAMP. Simply under alkaline conditions, without the inclusion of the metal-ion catalysts, the hydrolysis of 3', 3'-cGAMP (see Scheme 7) should look similar to hydrolysis of the RNA model, UpG (see Scheme 6). Both cyclic-di-AMP and 3', 3'-cGAMP have homologous structures, with the only difference being one of the two nucleotide bases for each molecule. Under alkaline conditions, cyclic-di-AMP is known to cleave by a first-order reach in OH^- concentration (Ora et al, 2013). The hydrolysis mechanism of cyclic-di-AMP begins with an intramolecular attack on the phosphorus by the 2'-alkoxide ion (Ora et al, 2013). A penta-coordinated phosphorane intermediate forms that is too unstable to pseudorotate and, as a result, the initial nucleophilic attack allows for the 'in-line' departure of the 5'-oxyanion (Ora et al, 2013). Both the linear cyclic-AMP dinucleotide and all 2', 3'-cyclic dinucleotide intermediates are known to hydrolyze at a fast rate (Ora et al, 2013) relative to the 3', 3'-cGAMP and DNA. As an intermediate, 2', 3'-cAMP does not seem to accumulate and quickly hydrolyzes to a mixture

of 2'-AMP and 3'-AMP (Ora et al, 2013). This reaction scheme can be similar to the reaction scheme for the phosphodiester cleavage of 3', 3'-cGAMP. Unlike RNA, no metal-ion-based model studies have been done on cyclic-di-NMP systems. In addition, there have been no studies done on 2', 3'-cyclic-di-NMP systems. Eventually, this research will explore a 2', 3'-cyclic dinucleotide model, and compare it with the 3', 3'-cyclic dinucleotide model.

Due to the arrangement of the nucleotide bases and phosphodiester bonds, four products are expected from the cleavage of all of the phosphodiester bonds found in 3', 3'-cGAMP, under basic conditions. Whether or not intermediates accumulate during the hydrolytic reaction will indicate whether the step, in the mechanism, leading to the intermediates, is fast or slow. We will specifically be able to determine whether the metal-ion of choice speeds 2'-OH intramolecular attack. The mechanism by which 3', 3'-cGAMP hydrolyzes can be compared to the mechanisms by which other biological molecules with phosphodiester bonds, such as RNA and DNA molecules, hydrolyze. An aqueous model system will be used to mimic the reaction between the secondary messenger molecule and the metal ions. The metal-ion of choice is Ca^{2+}, because it is particularly soluble at high pH. Under alkaline conditions, the 2'-OH group in RNA is first deprotonated (Lönnberg, 2011). The consequent 2'-oxyanion attacks the phosphorus atom and breaks down the phosphorane intermediate (Lönnberg, 2011). Meanwhile, the 5'-linked nucleosides that was formed leaves as an oxyanion (Lönnberg, 2011). Whether or not the deprotonated 2'-hydroxyl groups, of the di-cyclic secondary messenger, attack intramolecularly, such as with RNA, will be determined by the conclusion of this project. One of the main purposes of this project is to simply observe the kinetics of the phosphodiester cleavage and not have to worry about any other products formed as a result of pseudorotation or isomerization, which are typically seen when the pH conditions of the system are acidic.

Once the kinetic mechanism of the phosphodiester hydrolysis of 3', 3'-cGAMP has been determined, this research project can compare the kinetic mechanisms between 3', 3'-cGAMP and 2', 3'-cGAMP. The different phosphate linkages between both cyclic molecules may or may not have an effect on the kinetic mechanism. One would expect to see the same products formed, from the phosphodiester hydrolysis of 3', 3'-cGAMP, as a result of the phosphodiester hydrolysis of 2', 3'-cGAMP. However, the proximity of the free hydroxyl group to the phosphate, may lead to a different kinetic mechanism and, consequently, different products formed. Considering not a lot of research studies have been done on the hydrolysis of 2', 3'-cGAMP, or even 3', 3'-cGAMP, the kinetic studies that will be explored for both molecules can elucidate information on how the di-cyclic nucleotide structure and slight differences with the phosphate linkages can have an effect on the phosphodiester hydrolysis mechanism for each molecule.

The experiment reported in this research project discusses the effects of metal-ions, utilized as catalysts, that lower the energy barrier of the hydrolytic reaction of phosphodiester bonds found in 3', 3'-cGAMP and in 2', 3'-cGAMP. This project will explore how metal-ions behave in the mechanism by which phosphodiester bonds, specifically those found on 3', 3'-cGAMP and on 2', 3'-cGAMP, hydrolyze. Determining whether 3', 3'-cGAMP hydrolyzes via single-metal-ion mechanism or two-metal-ion mechanism can elucidate information on whether 3', 3'-cGAMP hydrolyzes in a manner that is similar either to RNA or DNA. Various analytical techniques will be performed to determine the identities of the 3', 3'-cGAMP- Ca^{2+} reactions and its overall hydrolysis reaction scheme. How the structure of the substrate and different phosphate linkages can have an effect on the mechanism will also be one of the main endeavors of this research.

Section B: Experimental

I. 3' ,3'-cGAMP and Ca^{2+} Reactions

500 nmol of 3',3'-cGAMP (cyclic [G(3',5')pA(3',5')p]) sodium salt (≥ 98% HPLC purified) was purchased from Sigma-Aldrich. All reactions contained 5 nmol of 3', 3'-cGAMP and 50 mM CAPS buffer of pH 11.5, totaling up to 500 µL of solution. $CaCl_2$ concentration varied from 0 – 0.33 M, and NaCl was added to maintain the ionic strength of 1.0. All reactions were maintained in a heat block at 37 ºC. To stop the reaction, also known as a "time-point", aliquots of the reaction mixture were added to 87.5 mM EPPS free acid (4-(2-Hydroxyethyl)-1-piperazinepropanesulfonic acid) (≥ 99.5% (titration)) or 87.6 mM HEPES (4-(2-Hydroxyethyl)piperazine-1-ethanesulfonic acid, N-(2-Hydroxyethyl)piperazine-N′-(2-ethanesulfonic acid)) and contained inside a micro-centrifuge tube. The EPPS and HEPES solutions are meant to stop the reaction by neutralizing the pH to about 7.00 or 8.00. The reactions were typically stopped at time-points: 2, 60, 120, 180, 240, 360, and 480 minutes. The aliquots were kept frozen until HPLC analysis.

II. HPLC Analysis

Samples were analyzed by reverse-phase HPLC. The HPLC model is Agilent 1100 Series. The nonpolar column that is used for the HPLC is a Bondclone™10 µm C18 148 Å, with an LC Column of size 300 x 3.9 mm. Thawed aliquots were injected into the HPLC, at a flow of 1.0 mL/min. The HPLC was set up with a nonpolar mobile phase (0.10 M ammonium acetate and 2.0% acetonitrile in millipore H_2O) that was isocratic for 0-15 minutes. For 15-30 minutes, the concentration gradient of Solvent B (95% H_2O, 5% acetonitrile) increases to 10%. The HPLC can be stopped at approximately 30 minutes for each injected aliquot. Using Agilent 1100 Series HPLC software, the absorbance peaks detected at 260 nm were integrated to find the area under those peaks.

A 3', 3'-cGAMP and Ca^{2+} (0.33 M) reaction, with a time-point of 3 hours, was performed to further confirm the identity of the one of its products, specifically the proposed 3'-AMP (adenosine 3'-monophosphate) product, that has an HPLC retention time of approximately 9 minutes. A second 3',3'-cGAMP and Ca^{2+} (0.33 M) reaction, with a time-point of 3 hours, was performed. 3'-AMP (2 μL) was added, or spiked, into the aliquot.

III. UV-Vis Spectrometry

The product peaks shown on HPLC were manually collected and analyzed through UV-vis spectroscopy. To maximize the amount of product collected, a separate $CaCl_2$ and 3',3'-cGAMP reaction was done. $CaCl_2$ stock solution (50 mM CAPS buffer of pH 11.5, millipore H_2O, and 0.33 M $CaCl_2$) was mixed into 3', 3'-cGAMP (5 nmol) to give a total of 120 μL 3',3'-cGAMP-Ca^{2+} reaction mixture. UV-vis spectra from 230 to 350 nm (analyzed for peak with retention time of 5 minutes) and from 230 nm to 350 nm (analyzed for peak with retention time of 9 minutes) were taken, using an Agilent Cary 60 UV-Visible Spectrophotometer.

IV. 2', 3'-cAMP and Ca^{2+} Reactions

2', 3'-cAMP and Ca^{2+} (0.33 M) reactions were performed to determine the retention times of the its known products, 2'-AMP and 3'-AMP. 2', 3'-cAMP (adenosine- 2',3'-cyclic monophosphate, sodium salt) was obtained from BioLog. All reactions contained 0.01 nmol of 2',3'-cAMP and 50 mM CAPS buffer of pH 11.5, totaling up to 500 μL of solution. $CaCl_2$ concentration varied from 0 – 0.33 M, and NaCl was added to maintain the ionic strength of 1.0. All reactions were maintained in a heat block at 37 ºC. To stop the reaction aliquots of the reaction mixture were added to 87.5 mM EPPS free acid (4-(2-Hydroxyethyl)-1-piperazinepropanesulfonic acid) (≥ 99.5% (titration)) contained inside a micro-centrifuge tube. The EPPS solution is meant to stop the reaction by neutralizing the pH to about 7.00 or 8.00. The

reactions were typically stopped at time-points: 15, 30, 45, 60, 90, 105, and 120 seconds. The aliquots were kept frozen until HPLC analysis.

V. 2', 3'-cGAMP and Ca^{2+} Reactions

500 nmol of 2',3'-cGAMP (c[G(2',5')pA(3',5')p]) sodium salt (≥98% HPLC purified) was purchased from Sigma-Aldrich. A 2',3'-cGAMP and Ca^{2+} (0.33 M) reaction was performed and aliquots, were taken at 0.5, 1, 2, 3, 5, 15, 21, 30, 60, 90, 120, 215, 360-minute time-points. All reactions contained 0.01 nmol of 2',3'-cGAMP and 50 mM CAPS buffer of pH 11.5, totaling up to 500 μL of solution. $CaCl_2$ concentration of either 0.00 M or 0.33 M, and NaCl was added to maintain the ionic strength of 1.0. All reactions were maintained in a heat block at 37 ºC. To stop the reaction aliquots of the reaction mixture were added to 87.5 mM EPPS free acid (4-(2-Hydroxyethyl)-1-piperazinepropanesulfonic acid) (≥ 99.5% (titration)) contained inside a micro-centrifuge tube. The EPPS solution is meant to stop the reaction by neutralizing the pH to about 7.00 or 8.00. The reactions were typically stopped at the performed time-points. The aliquots were kept frozen until HPLC analysis.

VI. Kinetic Analysis

The rate constant for 3', 3'-cGAMP degradation (k_{obs}) was found by plotting the absorbance of the 3', 3'- cGAMP reactant remaining against time and by fitting it to a 1st order integrated rate lawn exponential decay plot (see Equation 1), using Kaleidagraph™.

Equation 1: $$A_t = A_0 e^{-kt}$$

In order to determine the binding affinity and saturating rate constants, the k_{obs} for each Ca^{2+} concentration was then graphed against the calcium-ion concentration and was fit to a rectangular hyperbola, which is our secondary plot, using Equation 2.

Equation 2: $$k_{obs} = \frac{k_{Ca} * [Ca^{2+}]}{K_D + [Ca^{2+}]} + k_0$$

The k_{Ca} constant is the saturating rate constant, K_D is the dissociation constant, and k_0 is the rate constant at 0 M Ca^{2+}.

The amount of the products that appeared at each time-pint were also fit to a first-order exponential growth equation, in order to determine the rate at which the products of the hydrolysis reaction appeared.

Equation 3: $$\frac{k_{Ca}}{k_0} = e^{\frac{\Delta\Delta G_{act}^{\ddagger}}{RT}}$$

The k_{Ca} represents the saturating rate constant, k_0 represents the initial rate constant, $\Delta\Delta G_{act}^{\ddagger}$ represents the change in the delta activation energy of a reaction, R represents the gas constant value, 8.31 J/mol•K, and T represents the temperature at which the reaction proceeds. Equation 3 is used to determine rate enhancement caused by the metal-ion catalyst. This equation was used to compare between different reactions, where the type of substrate or metal-ion may differ.

Equation 4: $$y = \frac{k_1[A]_0}{k_2 - k_1}(e^{-k_1 t} - e^{-k_2 t})$$

The variable, k_1, represents the rate constant of the first step in the reaction, and k_2 represents the rate constant of the second step in the reaction, and $[A]_0$ represents the initial amount of the product.

Equation 4 represents the equation for a sequential first-order for an intermediate. This equation was used to determine whether one of the products from the hydrolysis reaction represented a sequential first-order reaction. This equation was mainly used mainly for hydrolysis reactions, where the products appearing on the HPLC seem to be intermediates (see Figure 9). In the calcium-mediated hydrolysis reaction of 2', 3'-cGAMP, at a single time-point,

an intermediate appears (see Figure 9b) and then is then quickly consumed in the next reaction at another later time-point (see Figure 9c).

Equation 5: $[P] = [A]_0(1 - \frac{1}{k_2 - k_1}(k_2 e^{-k_2 t} - k_1 e^{-k_1 t})) + k_0$

The variable, [P], represents the amount of the product or intermediate remaining in the reaction. $[A]_0$ represents the initial amount of the product or intermediate when it first appeared in the reaction. The variable, k_1, represents the rate constant of the first step of the reaction, and k_2 represents the rate constant of the second step of the reaction. The variable, k_0, represents the initial rate constant. Because the rate constant for the hydrolysis of 2', 3'-cGAMP (see figure 10a) is 0.183 s^{-1}, this same value was used to replace k_1 when creating the curve fit for the intermediates and products formed from the hydrolysis reaction.

Section C: Results

I. 3', 3'-cGAMP Hydrolysis

3', 3'-cGAMP and 2', 3'-cAMP standards were taken using HPLC analysis, in order to determine the retention times of these substrates. The absorbance of these substrates are used to eventually determine the amount of substrate remaining over time, as the time-point increases.

a)

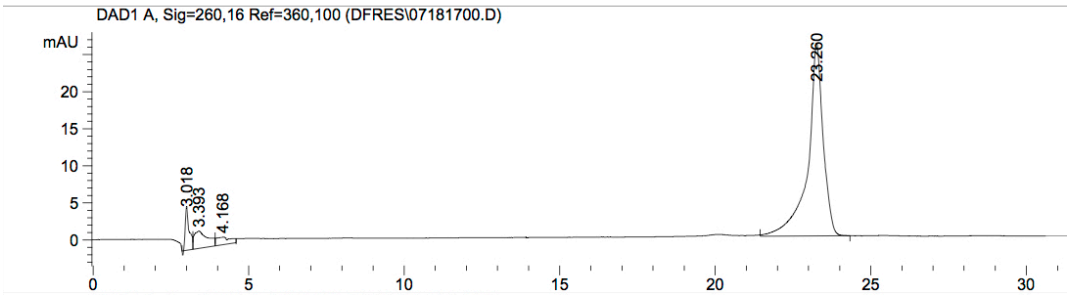

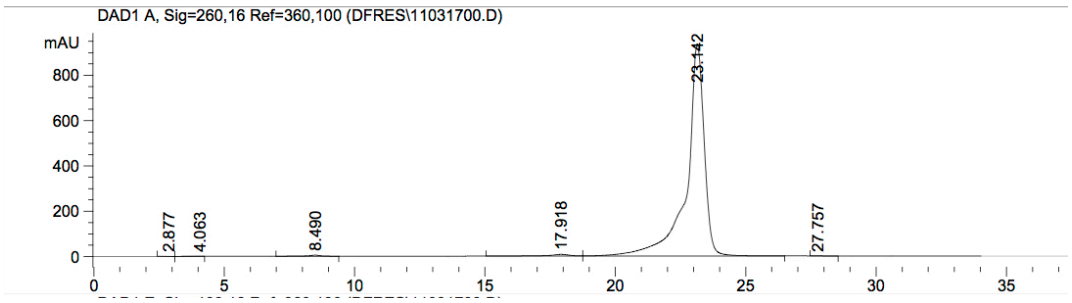

Figure 3: HPLC chromatographs of 3', 3'-cGAMP and 0 M Ca^{2+} with a time-point of 2 minutes (Figure 3a) and of a 2', 3'-cAMP standard (Figure 3b). For this sample, 3', 3'-cGAMP was introduced to aqueous solution conditions without any calcium solution and was injected into the HPLC to produce the chromatograph shown in Figure 3a. Only 2', 3'-cAMP, without any aqueous solution, was injected into the HPLC to produce the chromatograph shown in Figure 3b.

Figure 3 depicts no other products were formed and no consumption of the 3', 3'-cGAMP substrate. Moreover, 3', 3'-cGAMP has a retention time of approximately 23 minutes. 2', 3'-cAMP also has a retention time of approximately 23 minutes.

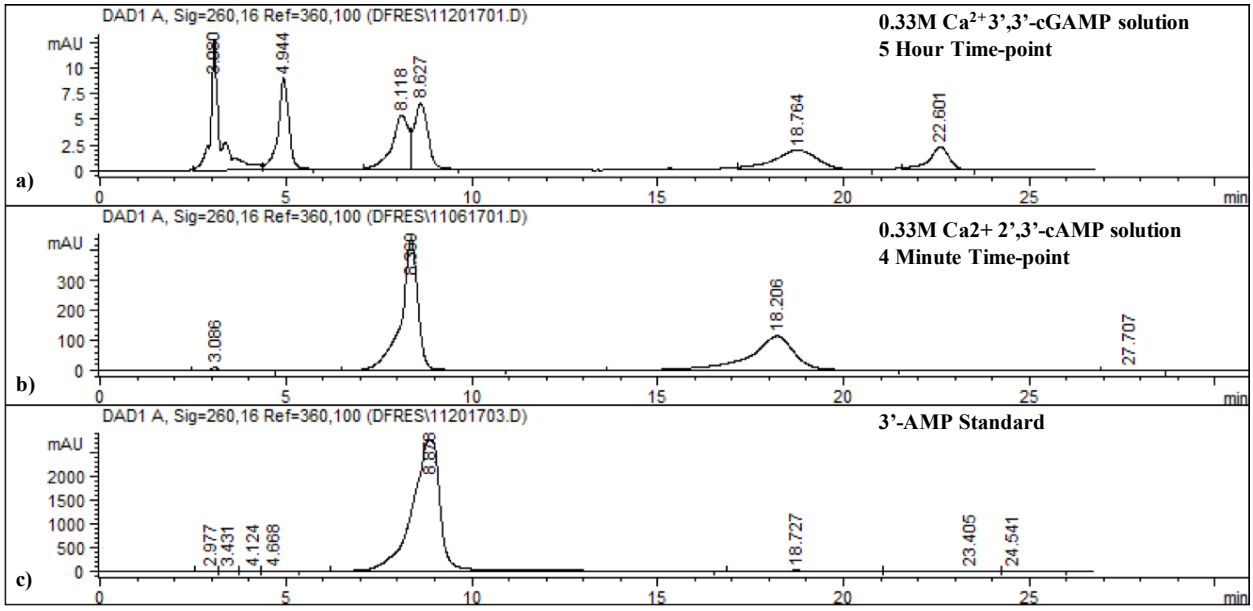

Figure 4: Reverse-phase HPLC chromatographs of 3', 3'-cGAMP reaction and standards used for identification of products. Figure 4a represents a 5-hour time-point of a 0.33 M $CaCl_2$ and 3', 3'-cGAMP solution mixture. In other words, the reaction between 0.33 M Ca^{2+} and 3', 3'-cGAMP ran for 5 hours. Figure 4b represents a 4-minute time-point of a 0.33 M $CaCl_2$ and 2', 3'-cAMP solution mixture. Figure 4c chromatograph represents a 3'-AMP standard.

The HPLC chromatographs provide analysis of products for the Ca^{2+}- 3', 3'-cGAMP reaction. According to Figure 4a, the four peaks at 5, 8, 9 and 18 minutes represent the four proposed products from the cleavage of 3', 3'-cGAMP with Ca^{2+} as the metal-ion catalyst. The peak at approximately 23 minutes is the 3', 3'-cGAMP peak, as determined by standards (see Figure 3a). According to Figure 3b, the two peaks at approximately 9 and 18 minutes represent the proposed products from the cleavage of 2', 3'-cAMP with Ca^{2+} as the metal-ion catalyst. Because no intermediates are observed in Figure 4a, the intermediates most likely do not include 2', 3'-cAMP, because, as seen in Figure 4b, letting the reaction occur for only 4 minutes, consumes all of the 2', 3'-cAMP. At approximately 4 minutes, the HPLC shows only the 3', 3'-cGAMP from the 3', 3'-cGAMP- Ca^{2+}. According to Figure 4c, the 3'-AMP has a retention time on the HPLC of approximately 9 minutes. As determined from the 3'-AMP standard (see Figure 4c), the peak with a retention time of approximately 9 minutes is the 3'-AMP cleaved product, while the other peak with a retention time of approximately 18 minutes is presumed to be the 2'-AMP cleaved product. The 2', 3'-cAMP is not observed on the chromatograph, where it has an expected retention time of approximately 23 minutes, as seen in Figure 4b, the absence of the 2', 3'-cAMP peak suggests that the molecule cleaves quickly.

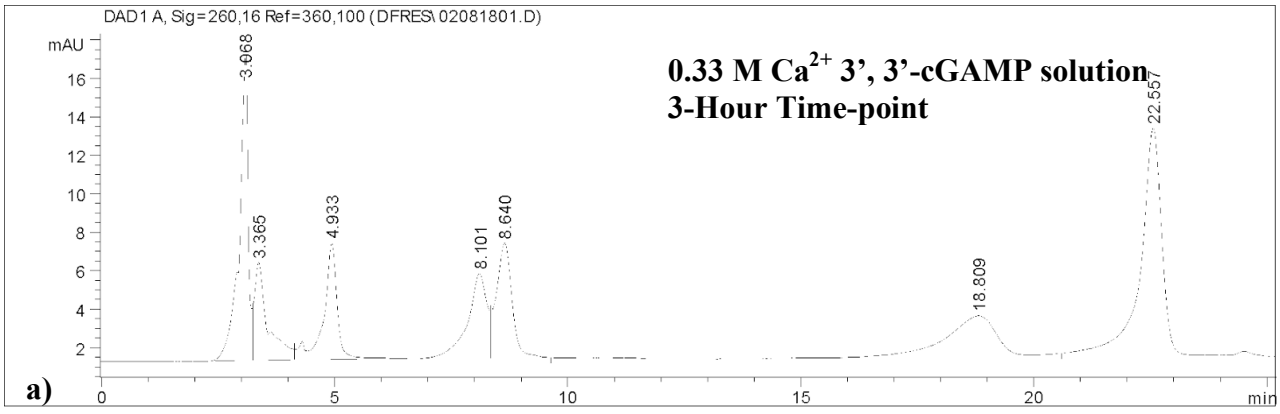

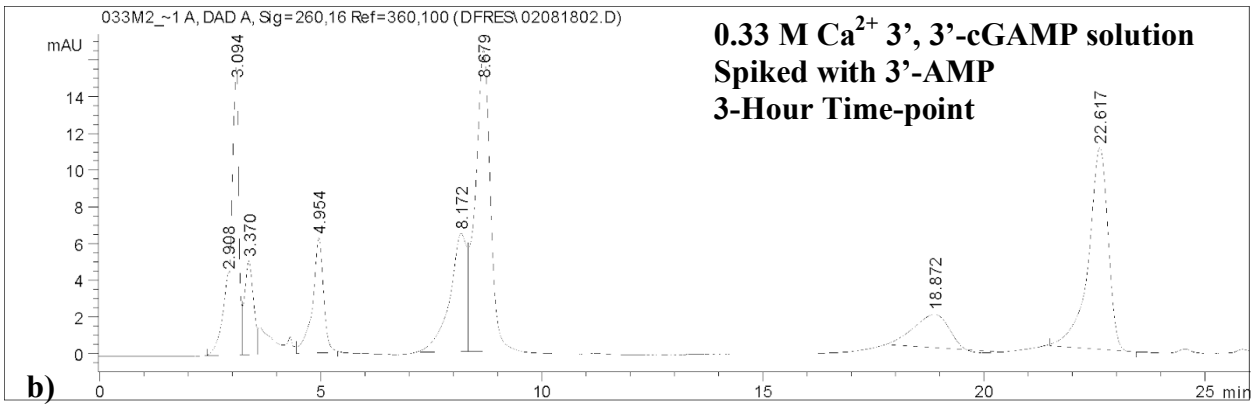

Figure 5: Reverse-phase HPLC chromatographs of 3',3'-cGAMP standards and identification of 3'-AMP product peak. Figure 5a represents a 3-hour time-point of a 3', 3'-cGAMP and 0.33 M Ca^{2+} reaction. Figure 5b represents a 3-hour time-point of a 3', 3'-cGAMP and 0.33 M Ca^{2+} reaction spiked with 2 µL of 3'-AMP.

Another set of 3', 3'-cGAMP and Ca^{2+} reactions were performed to further confirm the identity of the 8.6 minute (~ 9 minute) peak, which is one of the proposed products of the reaction. Both Figure 5a and Figure 5b are separate reactions that were both stopped at 3 hours. Moreover, the peaks in each of the two figures share the same identities. Figure 5a represents a standard chromatograph of a 3', 3'-cGAMP and Ca^{2+} reaction that was stopped at 3 hours. All four of the proposed products, with retention times of approximately 4.9, 8.1, 8.6 and 18.8 minutes, are shown on the graph, along with the 3', 3'-cGAMP reactant peak at approximately 22.6 minutes (see Figure 5a). Adding an additional 3'-AMP into a second 3', 3'-cGAMP and Ca^{2+} 3-hour time-point reaction increased the absorbance of the peak with a retention time of approximately 8.7 minutes (see Figure 5b). The major increase in absorbance confirms that the 8.7-minute peak (see Figure 5b), as well as the 8.6-minute peak (see Figure 5a), which is the retention time of 3'-AMP.

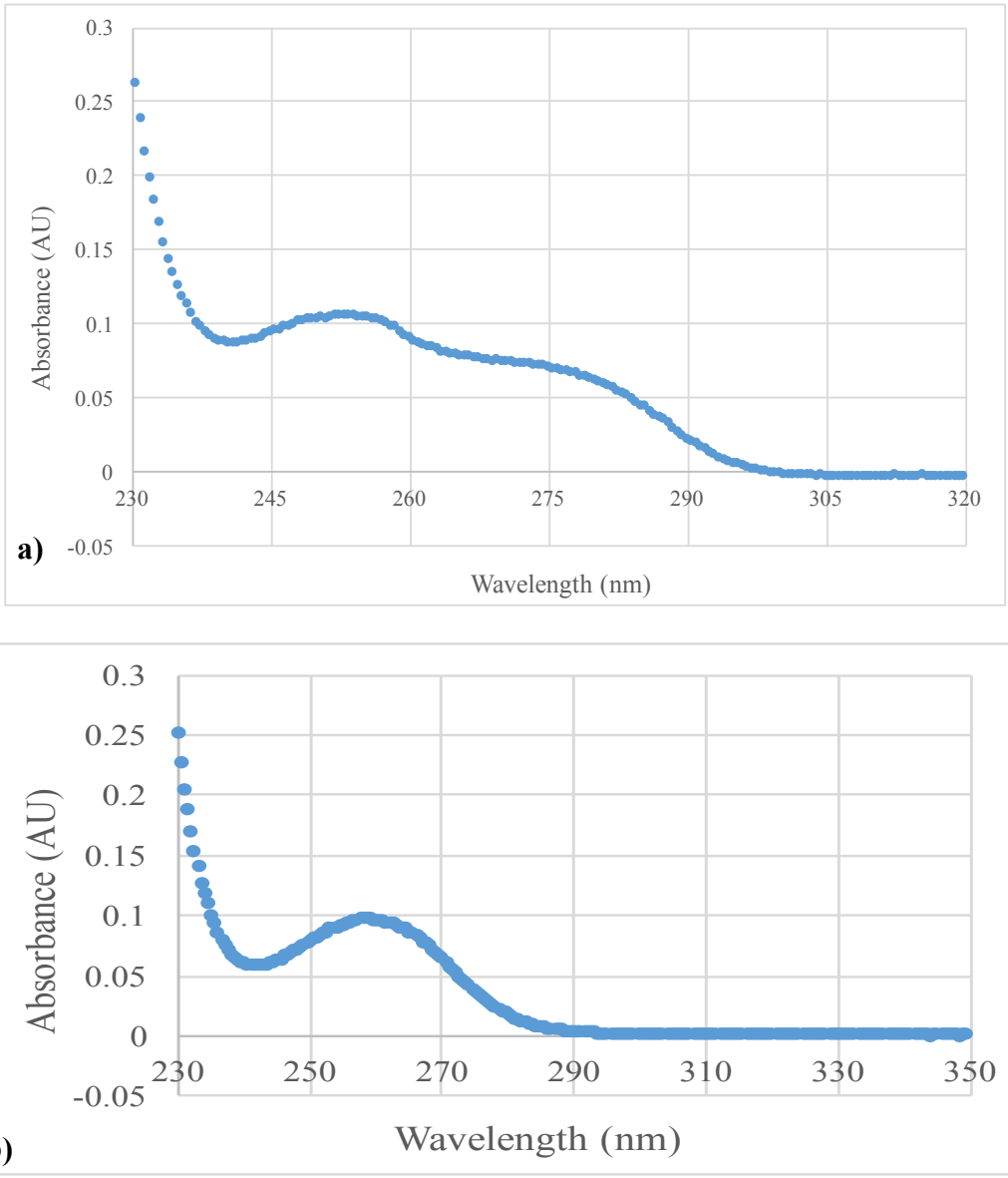

Figure 6: UV-visible spectra of individual components of reaction mixtures manually collected from HPLC. Figure 6a represents an early retention time peak at approximately 5 minutes, which was manually collected and then analyzed through UV-vis spectrometry. This product peak originated from 0.33 M Ca^{2+} and 3', 3'-cGAMP reaction mixture. Figure 6b represents a later retention time peak at approximately 9 minutes, which was manually collected from the HPLC.

The product peaks were further characterized by UV-vis spectroscopy. Figure 5a, which represents the peak with a retention time of about 5 minutes, displays a peak with two distinct humps. The guanosine standard is known to produce a peak that is slightly split into two humps, at a wavelength of 260 nm (Fischer, 1995). The two humps shown in Figure 6a indicate that the

product peak, which was manually collected from the HPLC, contains a guanosine nucleotide within its composition. Figure 5b displays a single large peak. The narrow and single-peak features suggests that the product sample that was manually collected from the HPLC contains an adenosine component, because the UV-vis spectrum of an adenosine standard also displays a large, narrow and single peak. The maximum absorbance is located at 260 nm, which is also characteristic of adenosine. The 3'-AMP standard chromatograph (see Figure 4c), as well as the reactions spiked with 3'-AMP (see Figure 5) further confirms that the peak with the retention time of approximately 9 minutes represents a 3'-AMP product that was cleaved from the 3', 3'-cGAMP substrate. Because the peak with a retention time of approximately 5 minutes contains a guanosine component, as displayed in Figure 6, the peak may represent either a 2'-GMP or a 3'-GMP product that was cleaved from the substrate. In addition, based on the order of the 3'-AMP and 2'-AMP peaks on the HPLC chromatograph, the 5 minute-peak most likely represents 3'-GMP, and the 8-minute peak most likely represents 2'-GMP.

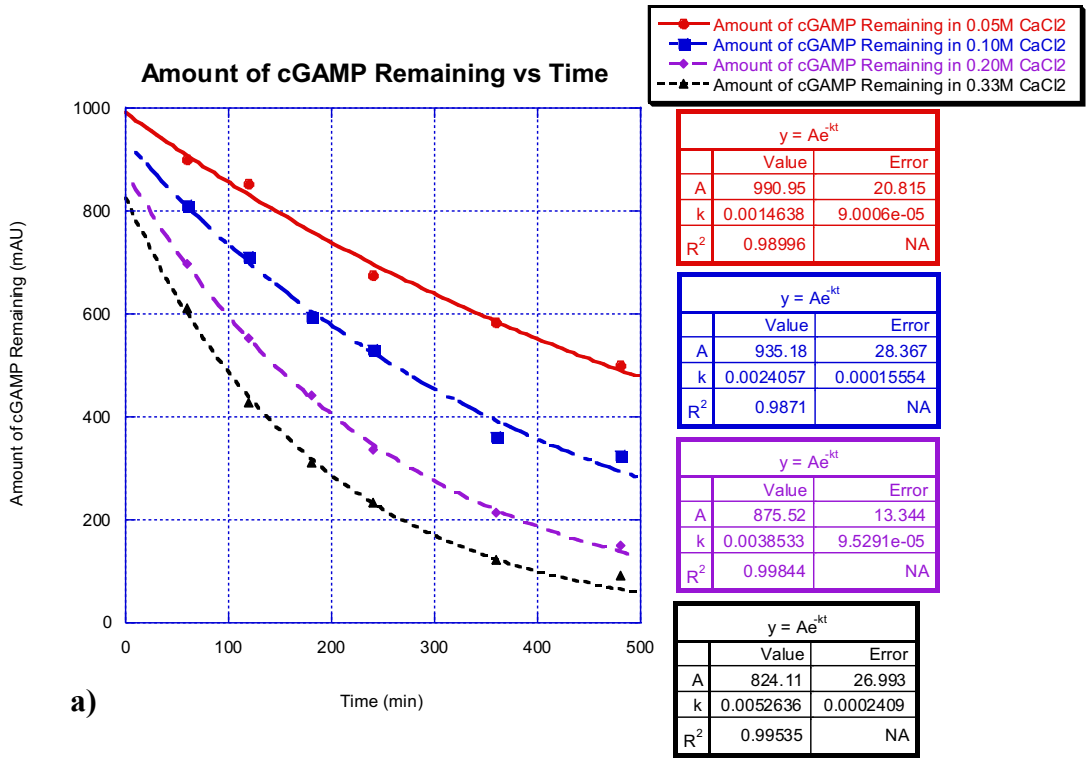

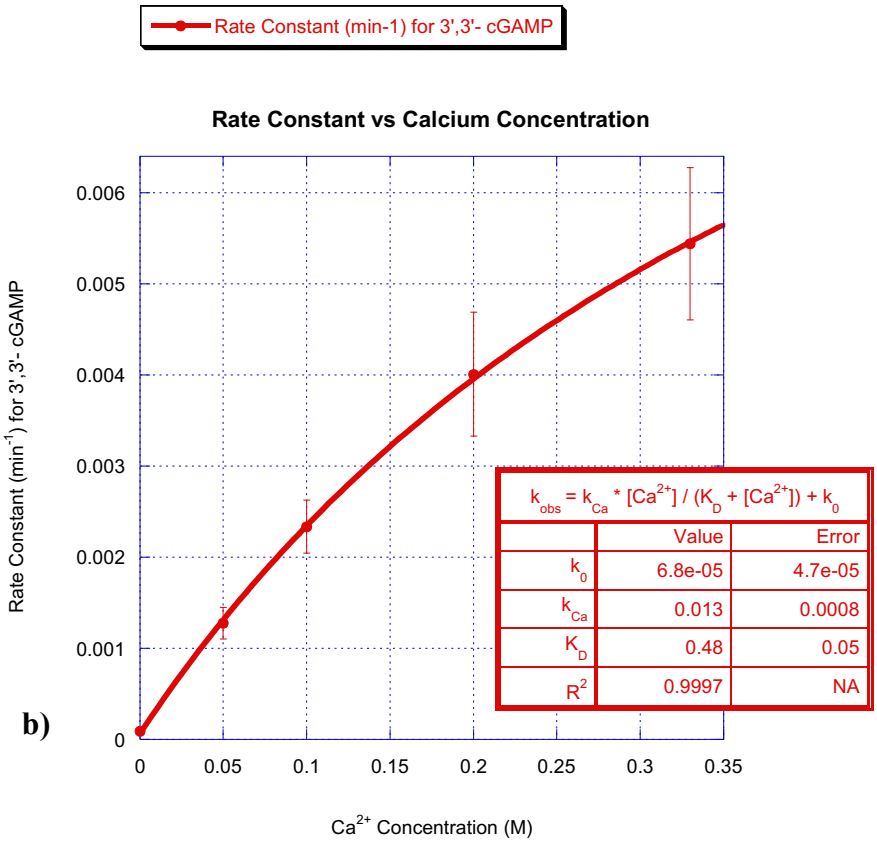

Figure 7: Primary and secondary plots obtained from Kaleidagraph™. Figure 7a represents the primary plot with the amount of Ca^{2+} concentration remaining as a function of time. Different Ca^{2+} concentrations are included in the primary plot. Using the exponential decay equation, rate constant values are obtained for each reaction containing a different Ca^{2+} concentration, using the following: 0.05 M Ca^{2+}, 0.10 M Ca^{2+}, 0.20 M Ca^{2+} and 0.33 M Ca^{2+}. Figure 7b represents the secondary plot with the second-order rate constants, which were obtained from the primary plot, plotted as a function of Ca^{2+} concentration. The rate constants plotted on the secondary plot are averages of rate constants obtained from three different trials. Using the observed rate constant as shown in the table of Figure 7b, values for k_0, the rate constant at which Ca^{2+} concentration is 0 M, k_{Ca}, the saturating rate constant and K_D, the dissociation constant were obtained. k_0 has a value of 6.8e-5 min^{-1}, k_{Ca} has a value of 0.013 min^{-1} and K_D has a value of 0.48.

According to the primary plot, the rate of cleavage of 3', 3'-cGAMP increases as the Ca^{2+} concentration increases. This increase in rate is due to an increased number of Ca^{2+} interacting and binding to the 3', 3'-cGAMP substrate. The bottom secondary plot shown in Figure 6 shows a rectangular hyperbola trend, which indicates that a single Ca^{2+} ion is being utilized in the reaction scheme, where the K_D value is 0.48 and k_{Ca} value is 0.013 min^{-1}. Using Equation 3 and

the values presented in Figure 7, with the k_{Ca}/ k_0 ratio value of approximately 191, R constant value of 8.31 J/mol•K, and temperature (T) value of 310 K, the $\Delta\Delta G_{act}^{\ddagger}$ value was determined to be approximately 13, 500 J/mol. The $\Delta\Delta G_{act}^{\ddagger}$ represents the change in free energy of the activation energy when Ca^{2+} is present in the reaction versus when it is not present in the reaction. The large $\Delta\Delta G_{act}^{\ddagger}$ suggests that the ΔG of the activation energy is decreased substantially when the single Ca^{2+} ion reacts with the 3', 3'-cGAMP substrate.

According to Figure 5, the steps leading to the formation and resolving of the intermediates, are very fast, because the intermediates cannot be seen on the HPLC – only the four final products (see Figure 3a). One of the intermediates that is suspected to form is 2',3'-cAMP. The rate at which 2',3'-cAMP is consumed is fast, because, according to Figure 3b), 2',3'-cAMP is no longer present – even at a short time frame.

II. 2', 3'-cGAMP Hydrolysis

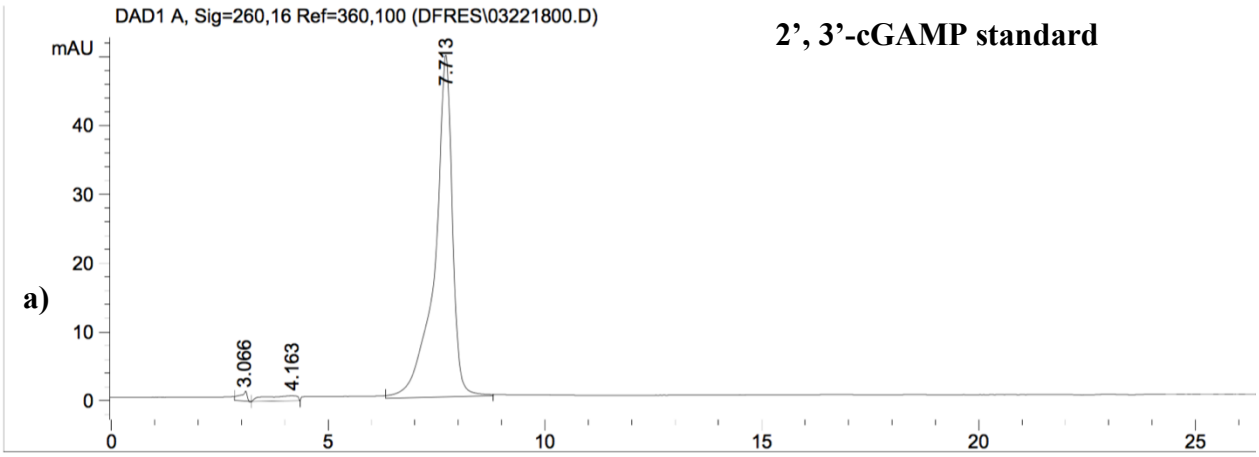

Figure 8: Reverse-phase HPLC chromatograph of a 2', 3'-cGAMP standard. 2', 3' has a retention time of approximately 7.7 minutes.

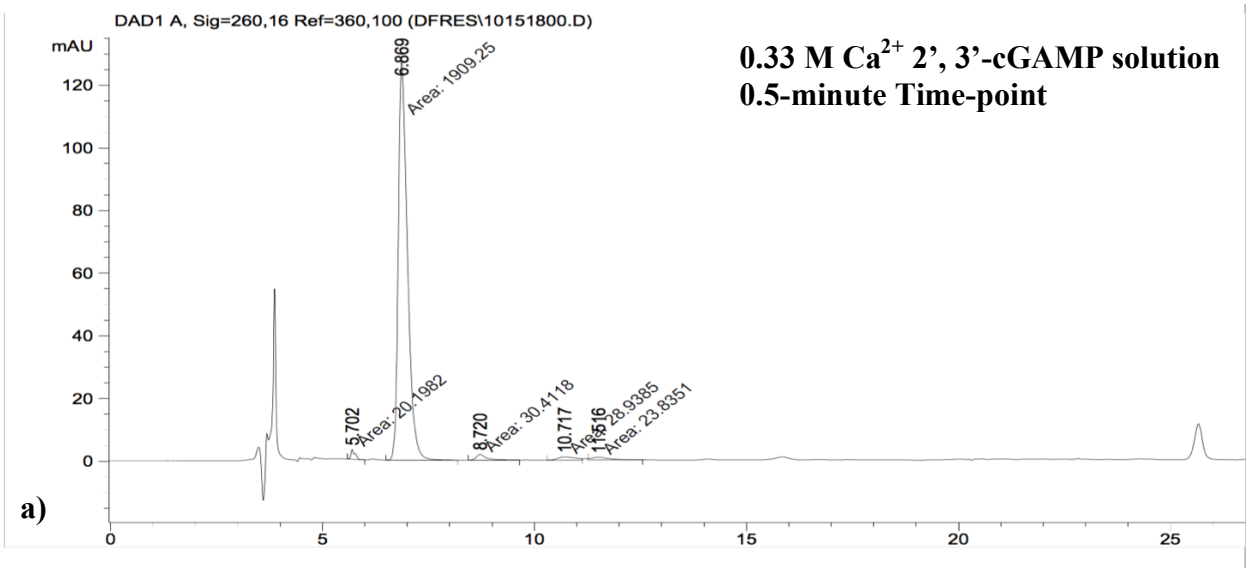
DAD1 A, Sig=260,16 Ref=360,100 (DFRES\10151800.D)
mAU
6.869
Area: 1909.25
5.702
Area: 20.1982
8.720
Area: 30.4118
10.717
Area: 28.9385
Area: 23.8351
0.33 M Ca2+ 2', 3'-cGAMP solution
0.5-minute Time-point
a)

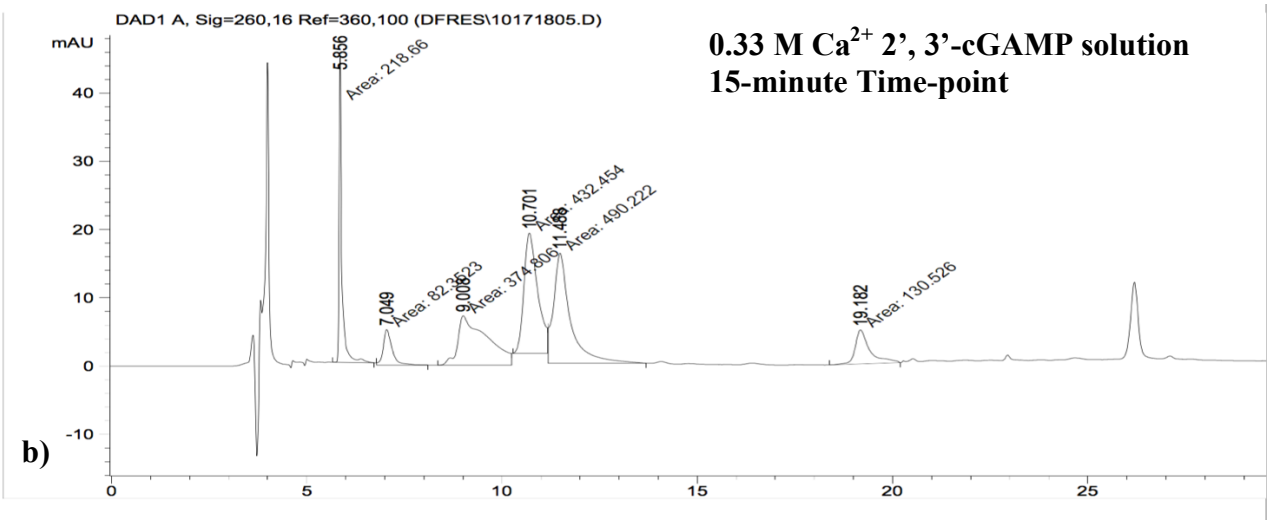
DAD1 A, Sig=260,16 Ref=360,100 (DFRES\10171805.D)
mAU
5.856
Area: 218.66
7.049
Area: 82.3623
9.008
Area: 374.806
10.701
Area: 432.454
Area: 490.222
19.182
Area: 130.526
0.33 M Ca2+ 2', 3'-cGAMP solution
15-minute Time-point
b)

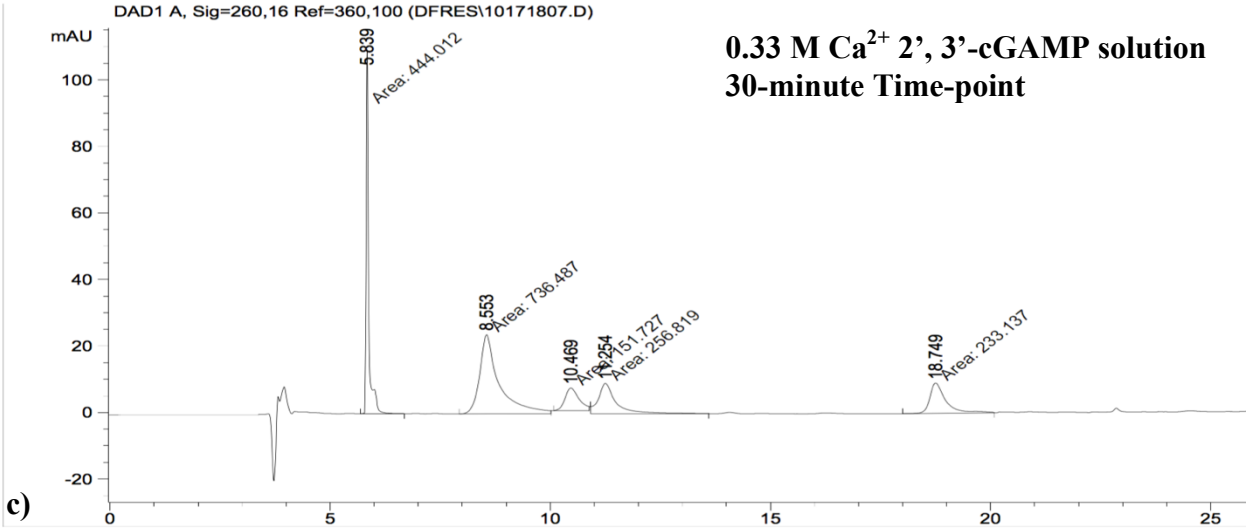
DAD1 A, Sig=260,16 Ref=360,100 (DFRES\10171807.D)
mAU
5.839
Area: 444.012
8.553
Area: 736.487
10.469
Area: 151.727
Area: 256.819
18.749
Area: 233.137
0.33 M Ca2+ 2', 3'-cGAMP solution
30-minute Time-point
c)

Figure 9: Reverse-phase HPLC chromatographs, at different time-points of 2', 3'-cGAMP in 0.33 Ca^{2+} solution. Figure 9a represents a 0.33 M Ca^{2+} and 2', 3'-cGAMP reaction that was stopped at 2 minutes. Figure 9b represents a 0.33 M Ca^{2+} and 2', 3'-cGAMP reaction that was stopped at 65 minutes. Figure 9c represents a 0.33 M Ca^{2+} and 2', 3'-cGAMP reaction that was stopped at 150 minutes.
(Note: The main products and/or intermediates presented with * notations).

A 2', 3'-cGAMP and Ca^{2+} reaction time-course was performed, and various aliquots with different time-points were taken. According to the 2', 3'-cGAMP standard (see Figure 8), the 2', 3'-cGAMP reactant peak should have a retention time of approximately 7-8 minutes. In Figure 9a, the peak with a retention time of approximately 7 minutes should be 2', 3'-cGAMP. Four other peaks with retention times of approximately 5.7, 8.7, 10.7 and 11.5 minutes appear. After letting the reaction run for 15 minutes, all of the proposed products from Figure 9a showed an increased area (see Figure 9b). A new product also formed by the 15-minute time-point, which has a retention time of approximately 18.7 minutes. After letting the reaction run for 30 minutes, the 2', 3'-cGAMP peak was no longer present (see Figure 9c). The products with the retention times of approximately 5.8, 8.6, and 18.7 minutes showed an increased area (see Figure 9c). However, the peaks with retention times of approximately 10.5 and 11.3 minutes showed a decrease in area (see figure 9c).

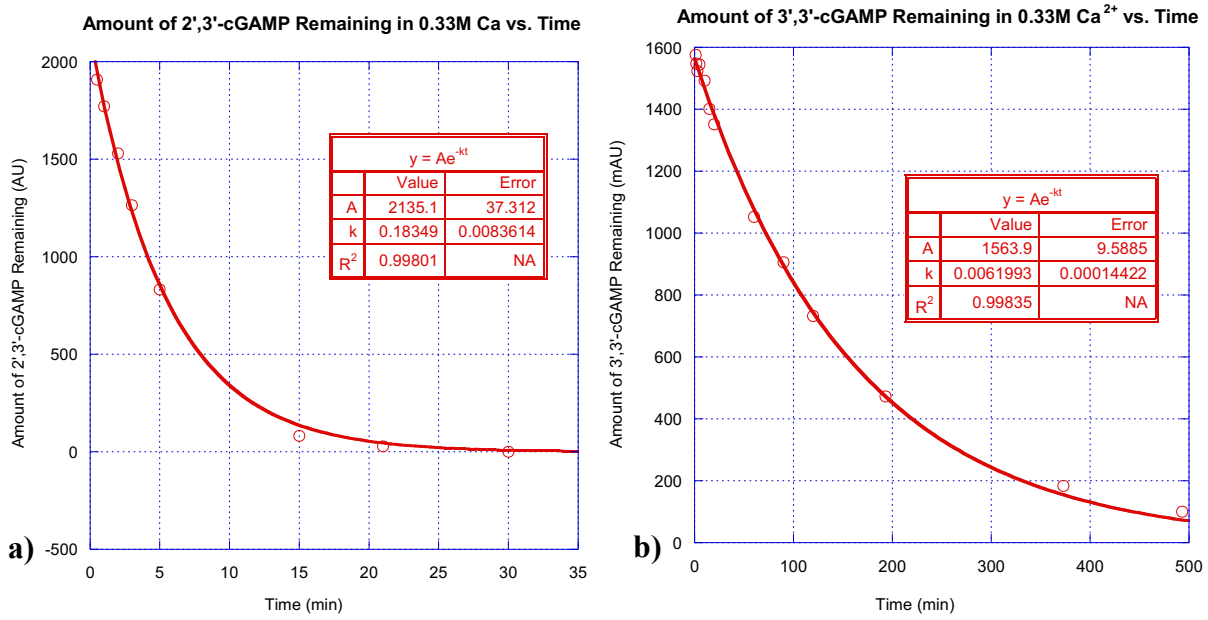

Figure 10: Primary plots obtained from Kaleidagraph™ for the reactant in the hydrolytic reaction. Figure 10a represents the amount of 2', 3'-cGAMP remaining as a function of time. Figure 10b represents the amount of 3', 3'-cGAMP remaining as a function of time. In each both sets of reactions, both the 2', 3'-cGAMP and 3', 3'-cGAMP substrates were saturated in a 0.33 M Ca^{2+} aqueous solution. Both graphs show an exponential decay model, where either substrate is hydrolyzed over a time course.

For one trial, the rate of hydrolysis of 2', 3'-cGAMP in a 0.33 M Ca^{2+} aqueous solution displays a rate constant, *k*, value of approximately 0.18 min^{-1}. A 3', 3'-cGAMP and 0.33 M Ca^{2+} reaction was set up as part of our control; each of the time-points for this reaction was immediately performed after each of our 2', 3'-cGAMP and 0.33 M Ca^{2+} time-points. The rate of hydrolysis of 3', 3'-cGAMP saturated in a 0.33 M Ca^{2+} aqueous solution displays a rate constant, *k*, value of approximately 0.0062 min^{-1}. The rate of hydrolysis of 2', 3'-cGAMP has approximately a 30-times fold greater than the rate of hydrolysis of 3', 3'-cGAMP.

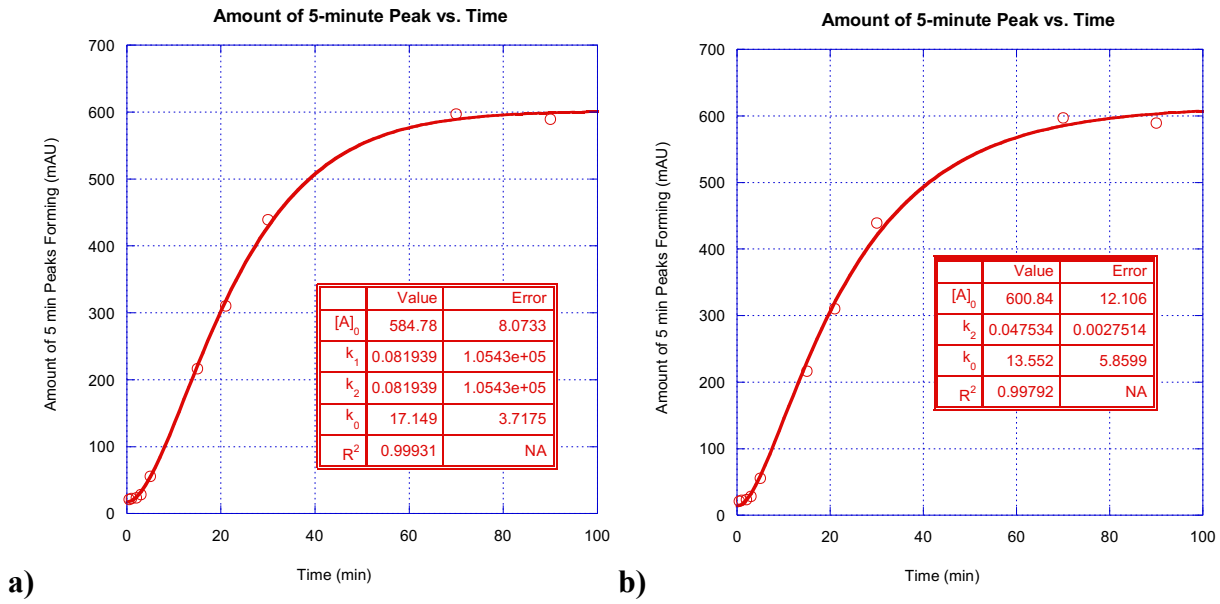

Figure 11: Primary plot obtained from Kaleidagraph™ for a product from the 2', 3'-cGAMP and 0.33 M Ca^{2+} hydrolytic reaction. The graph represents one of the products from the hydrolysis of 2', 3'-cGAMP saturated in a 0.33 M Ca^{2+} aqueous solution, which has a retention time of approximately 5 minutes on the HPLC. Figure 11 shows the data fitted onto Equation 5. Figure 11a does not have k_1 replaced by 0.183 min^{-1}, whereas Figure 11b does have the k_1 replaced by 0.183 min^{-1}.

For one trial, the hydrolytic reaction containing 2', 3'-cGAMP and 0.33 M Ca^{2+} produced a product. According to Figure 11, the amount of the product seems to be stabilizing by the 90-minute time-point. This observation may be due to the fact that the 10- and 11-minute peaks, shown on the HPLC chromatographs for the hydrolysis of 2', 3'-cGAMP, are gone after letting the reaction go for 90 minutes. In addition, from that same reaction, no new peaks are growing between the time-points of 90 – 360 minutes.

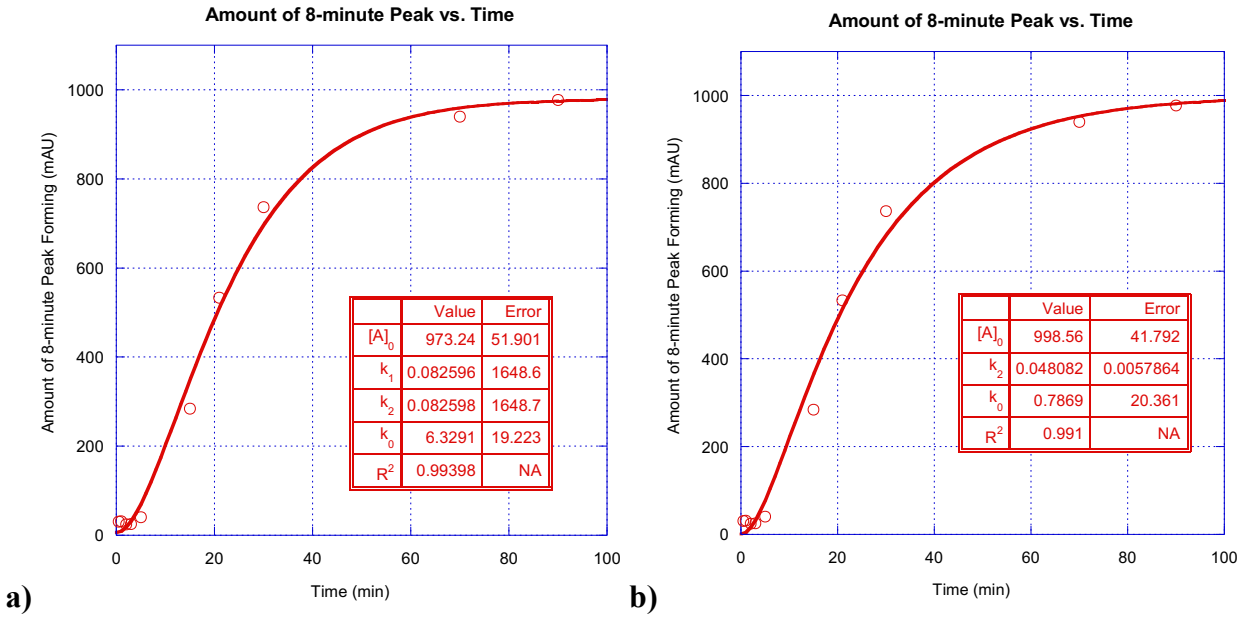

Figure 12: Primary plot obtained from Kaleidagraph™ for a product from the 2', 3'-cGAMP and 0.33 M Ca^{2+} hydrolytic reaction. This graph represents one of the products from the hydrolysis of 2', 3'-cGAMP saturated in a 0.33 M Ca^{2+} aqueous solution, which has retention time of approximately 8 minutes on the HPLC. Figure 12 shows the data fitted onto Equation 5. Figure 12a, does not have k_1 replaced by 0.183 min^{-1}, whereas Figure 12b does have the k_1 replaced by 0.183 min^{-1}.

During the same trial, the hydrolysis of 2', 3'-cGAMP produces a second product. According to Figure 12, the amount of product seems to be stabilizing by the 90-minute time-point. Masking the time-points after the 90-minute time-point creates an exponential growth curve (see Figure 12). This observation may be due to the fact that the 10- and 11-minute peaks, shown on the HPLC chromatographs for the hydrolysis of 2', 3'-cGAMP, are gone after letting the reaction go for 90 minutes. In addition, from that same reaction, no new peaks are growing between the time-points of 90 – 360 minutes.

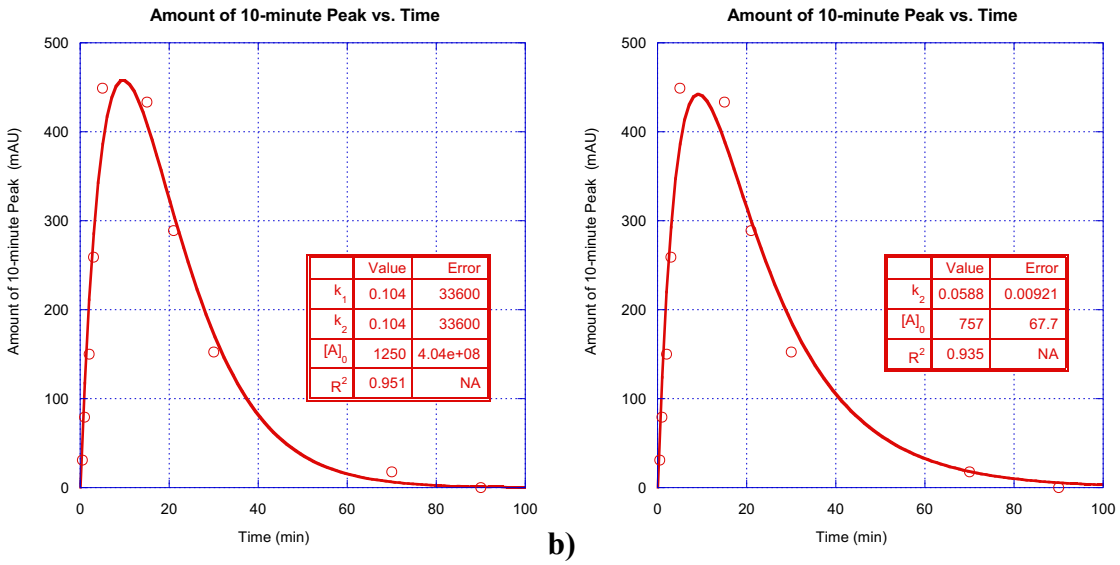

Figure 13: Primary plot obtained from Kaleidagraph™ for a product from the 2', 3'-cGAMP and 0.33 M Ca^{2+} hydrolytic reaction. This graph represents one of the possible intermediates from the hydrolysis of 2', 3'-cGAMP saturated in a 0.33 M Ca^{2+} aqueous solution, which has a retention time of approximately 10 minutes on the HPLC. This figure shows the data fitted on a sequential first-order reaction for an intermediate in a hydrolysis reaction (see Equation 4). Figure 13a, does not have k_1 replaced by 0.183 min^{-1}, whereas Figure 13b does have the k_1 replaced by 0.183 min^{-1}.

The hydrolysis of 2', 3'-cGAMP produces a proposed intermediate. The 10-minute peak was one of the peaks that appeared during the very early time-points, but then disappeared after letting the reaction proceed for 90 minutes.

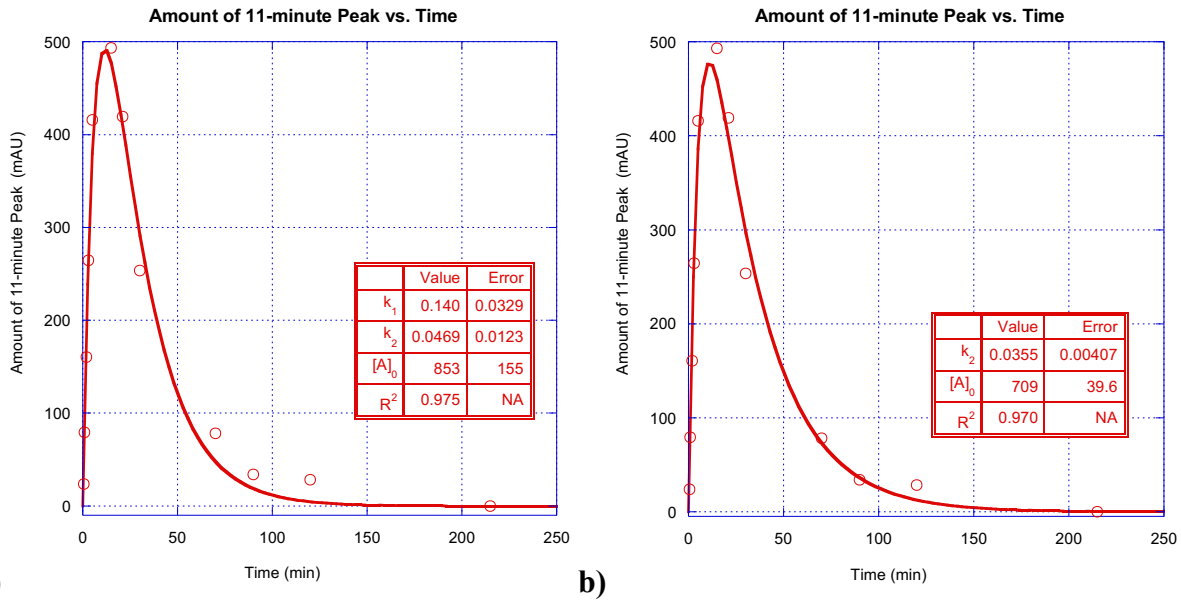

Figure 14: Primary plot obtained from Kaleidagraph™ for a product from the 2',3'-cGAMP and 0.33 M Ca^{2+} hydrolytic reaction. This graph represents one of the possible intermediates from the hydrolysis of 2',3'-cGAMP saturated in a 0.33 M Ca^{2+} aqueous solution, which has a retention time of approximately 11 minutes on the HPLC. This figure shows the data fitted on a sequential first-order reaction for an intermediate in the hydrolysis reaction (see Equation 4). Figure 14a, does not have k_1 replaced by 0.183 min^{-1}, whereas Figure 14b does have the k_1 replaced by 0.183 min^{-1}.

The hydrolysis of 2', 3'-cGAMP produces a second proposed intermediate. The 11-minute peak was one of the peaks that appeared during the very early time-points, but then disappeared after letting the reaction proceed for 90 minutes.

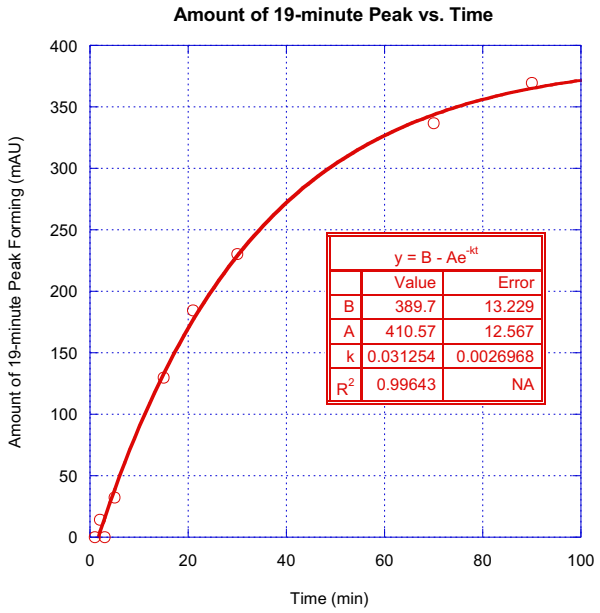

Figure 15: Primary plot obtained from Kaleidagraph™ for one of the products from the 2', 3'-cGAMP and 0.33 M Ca^{2+} hydrolytic reaction. This graph represents one of the products from the hydrolysis of 2', 3'-cGAMP saturated in a 0.33 M Ca^{2+} aqueous solution, which has retention time of approximately 19 minutes on the HPLC. Figure 15 shows the data fitted on an exponential growth equation (displayed on equation chart in Figure 15) up until the 90-minute time-point.

The hydrolysis of 2', 3'-cGAMP produces a third product. Masking the time-points after the 90-minute time-point creates an exponential growth curve (see Figure 15), which produces a rate constant of approximately 0.03123 min^{-1}.

Section D: Discussion

I. 3', 3'-cGAMP Analysis

The mechanism by which 3', 3'-cGAMP, a signaling molecule, hydrolyzes can be compared alongside with the enzyme-catalyzed hydrolysis mechanisms of other biological molecules, such as RNA and DNA. The usage of aqueous model system can help uncover the mechanism by which 3', 3'-cGAMP hydrolyzes. Due to the lack of research on the hydrolysis mechanism of 3', 3'-cGAMP, known hydrolysis mechanisms of other cyclic-dinucleotide models can be used as a basis for this current research. Cyclic-di-AMP, for instance, is another cyclic-dinucleotide whose

phosphodiesterase, like the phosphodiesterase of 3', 3'-cGAMP, belongs to the EAL domain. Because both cyclic-dinucleotide molecules are similar in structure, the mechanism by which 3', 3'-cGAMP is suggested to appear similar to the mechanism by which cyclic-di-AMP hydrolyzes (Scheme 2).

Unlike cyclic-di-AMP, 3', 3'-cGAMP contains two different nucleotide bases and, therefore, four different products should be produced when the molecule is hydrolyzed. The HPLC and UV-vis spectroscopy data suggest that four different products are indeed being produced when calcium is introduced into the system. According to Figure 7a, the rate at which 3', 3'-cGAMP hydrolyzes increases as the concentration of Ca^{2+} increases, which also proves that the Ca^{2+} contributes to the enhancement of the rate of hydrolysis.

Plotting the rate constants, which were obtained from primary plots, as a function of Ca^{2+} concentration (see Figure 7b) yields a rectangular hyperbola trend. This rectangular hyperbola, or downward curve shape, is consistent with RNA cleavage, where a single metal-ion is involved in the mechanism (Messina, 2014). Moreover, the single Ca^{2+} metal-ion is suggested to interact with the non-bridging oxygen atoms on the phosphate group of 3', 3'-cGAMP, which is the same mechanism observed with RNA and Ca^{2+} (Messina, 2014).

Because 3', 3'-cGAMP contains an internal nucleophile, like RNA, it can also begin its hydrolytic reaction with the intramolecular attack on its phosphorus atom. The mechanisms observed in Figure 16 are examples of electrophilic catalysis. The three phosphodiester models are the electrophiles, meanwhile the hydroxide-ion, or the internal deprotonated 2'-hydroxyl groups, are the nucleophiles. According to the single-metal-ion-mechanism by which an RNA model hydrolyzes, the initial cleavage step is kinetically slow (Messina et al, 2014). Because 3', 3'-cGAMP behaves like RNA, the initial cleavage of 3', 3'-cGAMP is also suggested to be a

slow step (see Figure 17 below). Moreover, the initial cleavage step in 3', 3'-cGAMP, like in UpG, is the rate-determining step of the overall hydrolytic reaction.

While the calcium-mediated hydrolysis reactions of 3', 3'-cGAMP and UpG each represent a single-metal-ion mechanism, the observed rate constants are different from each other by approximately a 10-fold difference. For instance, in a solution with a calcium concentration of 0.10 M, the observed rate constant for the hydrolysis of UpG is about 0.023 s^{-1} (Messina, 2014), while the observed rate constant for the hydrolysis of 3', 3'-cGAMP is about 0.0024 s^{-1} (Figure 7a). At a calcium concentration of 0.20 M, the observed rate constant for the hydrolysis of UpG is about 0.040 s^{-1} (Messina, 2014), while the observed rate constant for the hydrolysis of 3', 3'-cGAMP is about 0.0039 s^{-1} (Figure 7a). At a calcium concentration of 0.33 M, the observed rate constant for the hydrolysis of UpG is about 0.054 s^{-1} (Messina, 2014), while the observed rate constant for the hydrolysis of 3', 3'-cGAMP is about 0.0053 s^{-1} (Figure 7a). The numerical values of the observed rate constants for both molecules are very similar to each other, with the difference being that they are each different by a factor of 10. This 10-fold difference can suggest that di-cyclic structure of 3', 3'-cGAMP accounts for a slower rate of hydrolysis than for the UpG molecule.

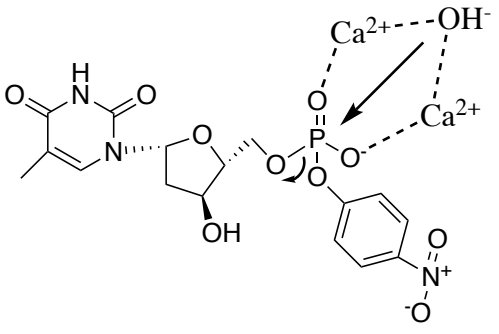

a)

(Adapted from Kirk et al, 2010)

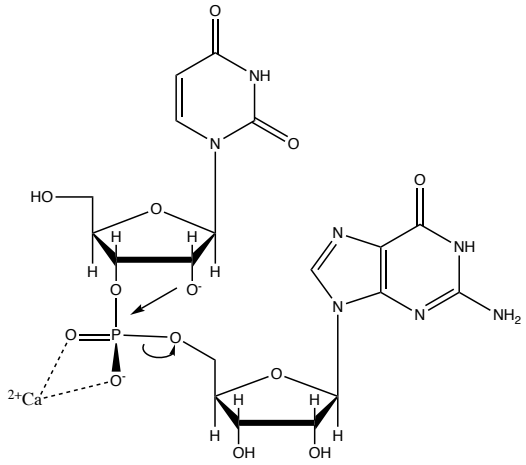

b)

(Adapted from Kyle Messina's Thesis)

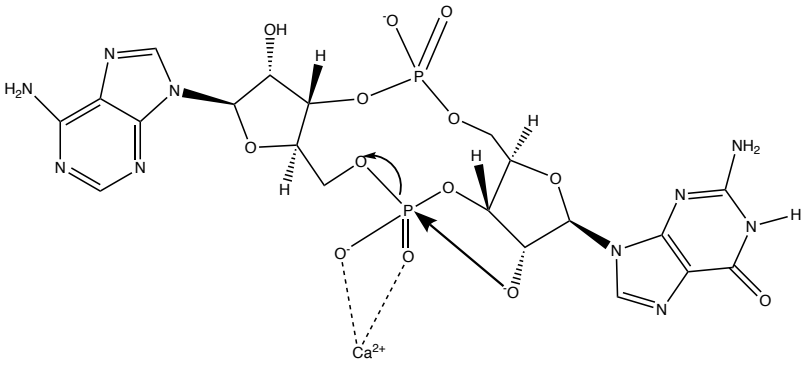

c)

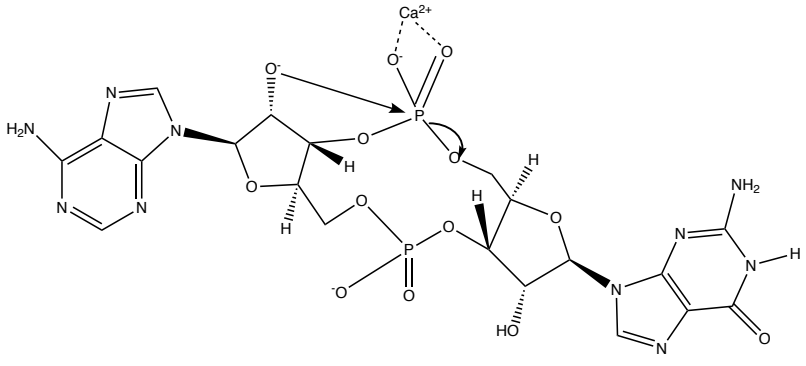

d)

Figure 16: General schemes of the hydrolytic reactions of 3', 3'-cGAMP, UpG and of T5PNP. Figure 16a represents a di-nuclear meal-ion mechanism, while Figures 16b, 16c and 16d represent a mononuclear metal-ion mechanism. Both Figures 16c and 16d represent the same mechanism scheme, except each of these figures present a nucleophilic attack by a 2'-OH that belongs to different nucleotide base.

Figures 16a-d depict biological molecules that each contain a set of phosphodiester bonds. The non-bridging oxygen atoms in each set of phosphodiester bonds are coordinated to a Ca^{2+} ion that allows for the nucleophilic attack on the electrophilic phosphorus. In the RNA model, 5-uridine-guanosine 3' (UpG), the 2'-hydroxyl can act as a nucleophile (see Figure 16b). Because the DNA model, T5PNP, does not have an internal nucleophile, however, the Ca^{2+} ion also coordinates with an external hydroxide ion that can behave as the nucleophile for the hydrolytic reaction (see Figure 16a).

In addition to their different mechanisms (or similar, when referring to 3',3'-cGAMP and UpG) the metal-ion(s) involved in each of the models have different energetic contributions to the hydrolysis mechanism.

	T5PNP (DNA model)	UpG (RNA model)	3',3'-cGAMP
$\Delta\Delta G_{act}^{\ddagger}$	**18 kJ/ mol TOTAL** • w/ 1st metal-ion: 12 kJ/mol • w/ 2nd metal-ion: 6 kJ/ mol	**14.9 kJ/ mol**	**13.5 kJ/ mol**
Rate Enhancement	**900X** (with two metal ions) * 90X with a single metal ion	**326X**	**191X**
# Metal Ions Used in Mechanism	**2**	**1**	**1**

*All of the values listed for T5PNP were obtained from Kirk et al, 2010 and the values obtained for UpG were obtained from Messina, 2014.

Table 1: Comparison of rate enhancement and $\Delta\Delta G_{act}^{\ddagger}$ values between T5PNP, UpG and 3', 3'-cGAMP. 3', 3'-cGAMP seems to have $\Delta\Delta G_{act}^{\ddagger}$ and rate enhancement values that are more similar to RNA than to DNA. T5PNP and UpG were also introduced to the same aqueous model system conditions as 3', 3'-cGAMP.

In terms of the energetic contributions of the catalytic metal-ions, 3', 3'-cGAMP appears to behave similarly to UpG. The $\Delta\Delta G_{act}^{\ddagger}$ values represent the difference in the change in activation energies when the phosphodiester substrate is in the presence of the metal-ion catalyst and when the substrate is not in the presence of the catalyst. The large $\Delta\Delta G_{act}^{\ddagger}$ values for T5PNP may be explained by the fact that DNA utilizes two metal-ions instead of one. However, the energetic contribution when a single metal-ion, instead of two metal-ions, contributes to the hydrolysis of T5PNP is similar to the values obtained from the single metal-ion mechanisms of UpG and of 3', 3'-cGAMP. The energetic contribution when only a single metal-ion coordinates with the non-bridging oxygen atoms of T5PNP and with hydroxide-ion nucleophile is 12 kJ/mol; the rate at which T5PNP hydrolyzes is enhanced 90 times when only a single metal-ion is involved in the mechanism. Moreover, the energetic contribution and rate enhancement when T5PNP utilizes only a single metal-ion are more similar to the values obtained for UpG and for 3', 3'-cGAMP than the values obtained for T5PNP, when both of its metal-ions are involved in its hydrolytic reaction.

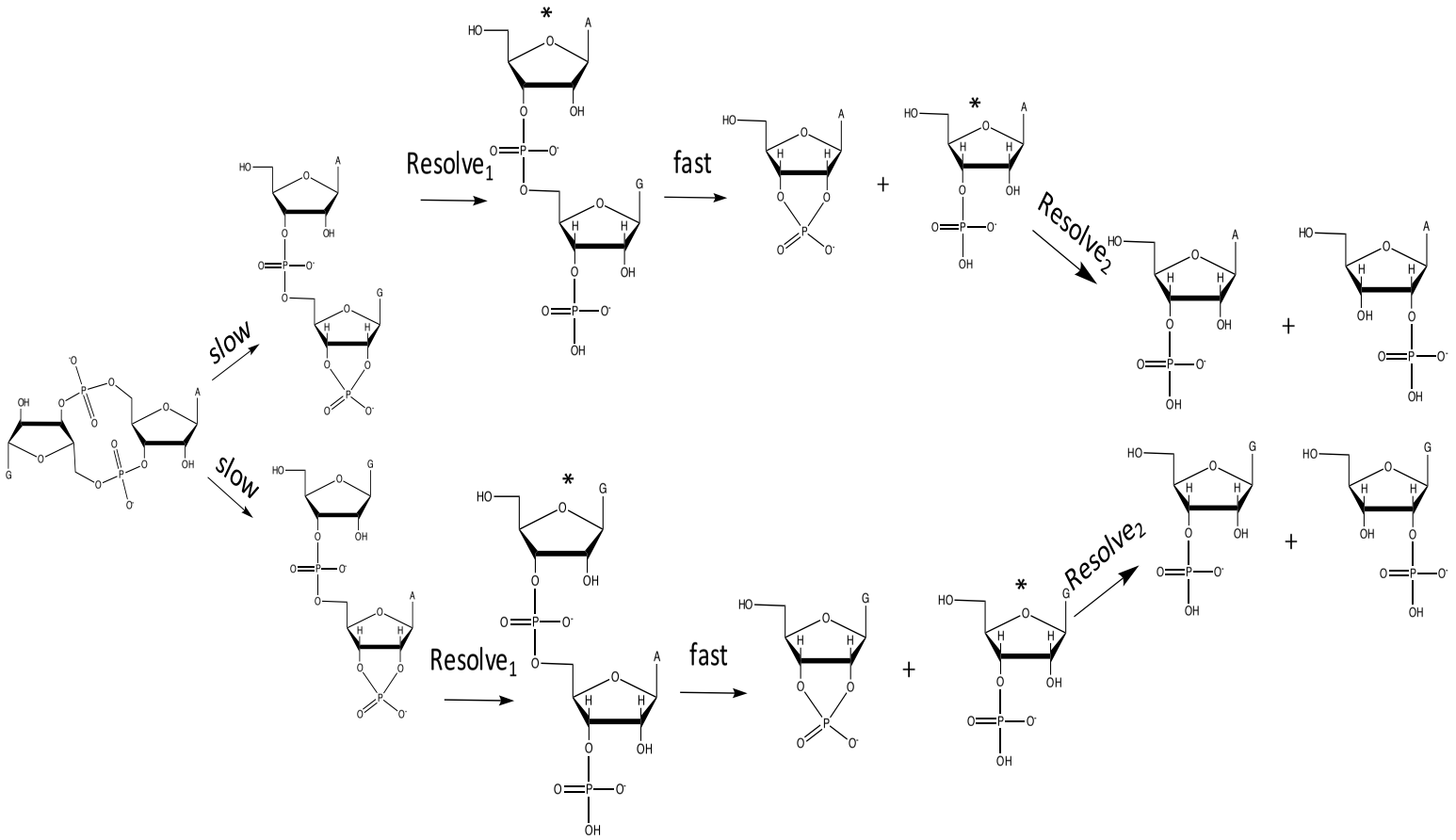

Figure 17: Reaction scheme of the hydrolysis of 3', 3'-cGAMP. Knowing that 3',3'-cGAMP hydrolyzes in a similar manner as RNA, like with RNA, the initial cleavage of the 3',3'-cGAMP substrate is suggested to be slow, while the step after the 1st resolve is suggested to be fast. A mixture of four different products are cleaved as a result of the hydrolytic reaction.
(* represents a mixture of 2'and 3' products, where only 3' products are shown).

The fact that previous research studies claim that the EAL-domain phosphodiesterases hydrolyze 3', 3'-cGAMP via two-metal-ion mechanism, suggests that the aqueous conditions introduced in this study, versus the conditions that are similar to actual enzyme-active sites, may have an effect on the type of mechanism that occurs for the hydrolytic reaction of the cyclic-dinucleotide molecule. According to the values shown in Table 1, a single metal-ion that interacts with two sets of phosphodiester bonds may not provide as much catalytic rate enhancement as a single metal-ion that interacts with only a single set of phosphodiester bonds. Energy coordinate diagrams that display the steps leading to the phosphodiester bond cleavage of 3', 3'-cGAMP can give some insight on the necessity of having high enhancement rates in order to increase the hydrolysis rate.

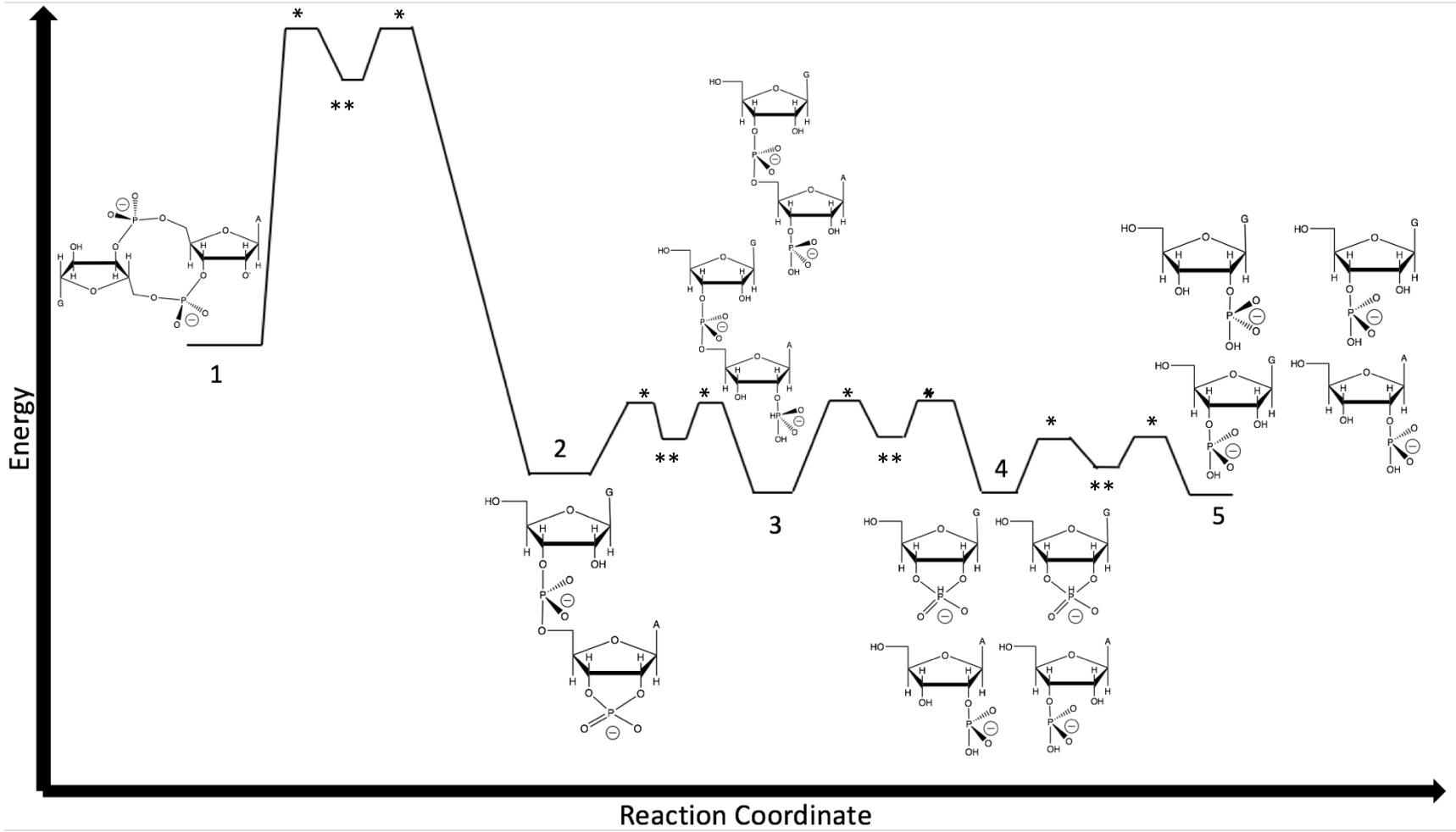

Figure 18a: Energy diagram of the hydrolysis reaction of 3', 3'-cGAMP. The reactant (1) starts out as a di-cyclic molecule, which has phosphates whose non-bridging oxygen atoms share a negative charge. After the first cleavage, the reactant becomes linearized (2). After an attack on the phosphorus of the 2'-3'-linked phosphate (2) by a hydroxide ion found in the basic solution, the reaction proceeds to resolve into two isomers of another linearized product (3), with the added oxygen atom bonded to the phosphorus. After phosphodiester cleavage of both linear products, the reaction proceeds to form four products: two products with a single guanosine base and two products with a single adenosine base (4). After the two products, with a 2'-3'-linked phosphate, resolve, the reaction ends with formation of four products: 3'-AMP, 2'-AMP, 3'-GMP, 2'-GMP (5).
(The * notes indicate a transition state, where phosphodiester bonds are either forming or breaking. The ** notes indicate a phosphorane intermediate.)

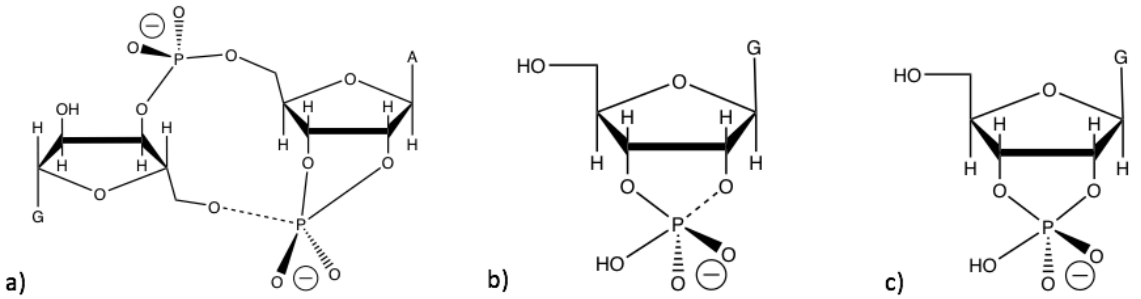

Figure 18b: Transition state and intermediate structures from the hydrolytic reaction of 3', 3'-cGAMP. The dashed line in the transition state (a) represents the bond breaking, which is the initial cleavage of the reaction. The dashed line in the transition state (b) represents the bond forming; this step is followed by the formation of a phosphorane intermediate (c).

Energy coordinate diagrams are useful in generally showing how a reaction progresses from reactants to products. According to Figure 18a, the initial step leading to the first linearized intermediate of the reaction has the highest energy barrier that needs to be overcome. Moreover, the necessity of an enzyme to increase the rate of hydrolysis is especially important for this initial step. An enzyme, or specifically a phosphodiesterase, would be especially important in lowering the energy barrier of the initial cleavage step. However, after the formation of the 2', 3'-cAMP, or the first linearized product, the following steps generally do not require as much energy. In other words, once 2', 3'-cAMP forms, the rest of the hydrolytic reaction of 3', 3'-cGAMP becomes thermodynamically favorable.

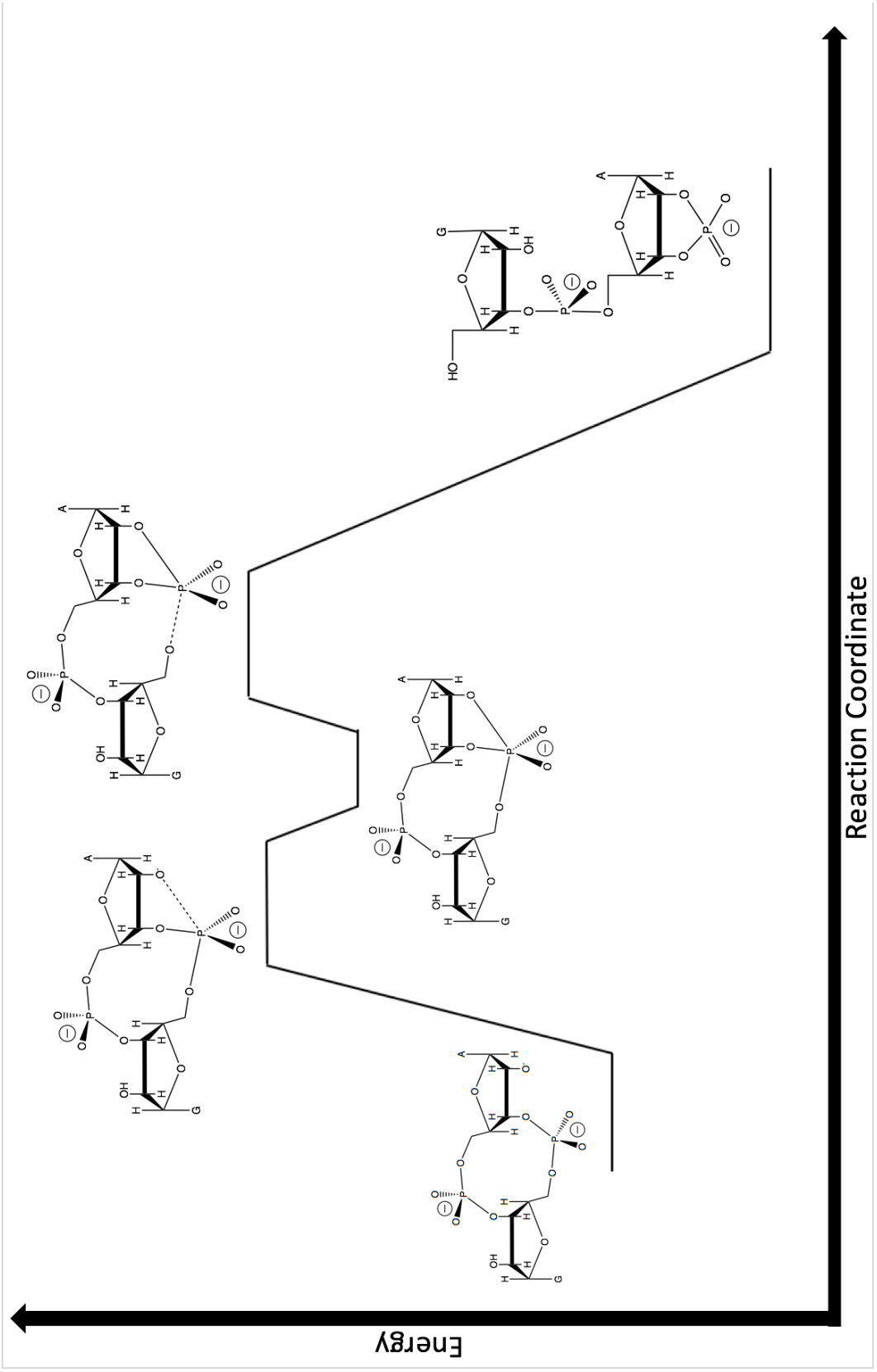

Figure 19: Energy diagram of the 3’,3’-cGAMP hydrolyzing into linear product. The energy diagram shows the reaction scheme leading to the linear product, 2’,3’-cAMP. This diagram also shows high transition states involving the formation and cleavage of phosphodiester bonds, as well as a short-lived phosphorane intermediate.

The initial cleavage step of 3', 3'-cGAMP should produce a linear intermediate, 2', 3'-cGAMP. After Ca^{2+} coordinates with the two non-bridging oxygen atoms that are both sharing a negative charge, the 2'-hydroxyl group attacks and forms a bond to the phosphorus atom and then creates a short-lived phosphorane intermediate, which cannot be detected by the HPLC (see Figure 19). The initial cleavage step begins after the first phosphorane intermediate, where the bond between the 5'-hydroxyl group of one of the nucleotide bases and the phosphorus center of the phosphodiester in the other nucleotide base breaks (see Figure 19). This step leading to the linear intermediate, 2', 3'-cAMP, as well as its accumulation, cannot be detected by the HPLC.

The hydrolytic reaction of 3', 3'-cGAMP seems to produce four products; however, whether or not any intermediates are being formed is still unclear. Because no intermediates are being seen on the HPLC, the overall cleavage step of the reaction is very slow. By the time the reaction proceeds to the linear product, 2', 3'-cAMP, the reaction had already proceeded to the next step before the HPLC can detect any detectable amount of the intermediate. Further research has to be done to determine the identity of the intermediates, which can be done by possibly lowering calcium concentrations or by lowering the pH concentrations so that the steps following the cleavage reaction can occur slower. One of the goals of this project is to be able to separate the two 8-minute peaks that are observed in the chromatograph for the 3', 3'-cGAMP hydrolytic reaction (see Figure 4a). Achieving separation of peaks is crucial for confirming the actual identities of the chromatograph peaks. However, modifications would have to be made to the HPLC in order to achieve good separation of peaks. Moreover, spiking the reaction with a possible and hypothesized product can be done to confirm the identities of peaks that show up on the chromatograph. Figure 5 is a good example of how spiking reactions can further confirm the identity of a peak.

II. 2', 3'-cGAMP Analysis

The rate of appearance of the observed products were obtained after integrating the areas under the proposed main product peaks from the hydrolytic reaction of 2', 3'-cGAMP, and graphing those areas to obtain primary plots. Despite being a combination of two possible products, the ~9-minute peak (see Figure 9b) was integrated altogether instead of being separated right in between the two "humps." According to Figure 10a, the rate constant for the initial breakdown of 2', 3'-cGAMP is 0.183 min^{-1}. The k_2 rate constants shown in Figures 11b, 12b, 13b, 14b, and 15 are all within the same range of approximately 0.03 – 0.05 min^{-1}. The fact that all of the k_2 values, after replacing k_1 with 0.183 min^{-1}, are within the same range, further proves that the products are appearing at about the same rate. For Figures 11, 12, and 15, each of the proposed products seem to be disappearing, instead of growing in the reaction mixture, after the letting the reaction run for 90 minutes. Furthermore, graphing the original data that includes the full time-course up until 360 minutes, using a sequential first-order equation for an intermediate, yields a good fit. Doing so for the 5, 8 and 19-minute peaks, yield reliable R^2 values, as well as k_1 and k_2 values that are within the same range from each other. However, because the reactants should be increasing in absorbance or area, the data points following the 90-minute time-point, which is the time before the absorbance for each time-point started decreasing, were masked and fitted to an exponential growth equation. These graphs also yield reliable R^2 values, as well as k values that are within the same region from each other. The decrease in product is unusual, because as the time-points increase, the amount of reactant should be decreasing, while the amount of product should be increasing. A possible explanation for the decrease in product after 90 minutes could be that the products are being consumed in a side reaction.

According to Figures 13 and 14, the data points fit a clear graph of an intermediate, where the product appears and then disappears at some point during the middle of the reaction. Both Figures 13 and 14 appeared close to each other on the HPLC chromatographs. As result, the rate constants may not be so reliable, because some amount of one of the peaks may be combining into its neighboring peak. Achieving a good separation between the 10- and 11-minute peaks would be helpful in obtaining more accurate rate constants. Overall, using the sequential first-order equation, the rate constants for the formation of both intermediates are at least 10-times greater than the rate constants for the formation of the other three main products, also using the sequential first-order equation. These 10- and 11-minute peaks appear more similar to actual intermediates, than the other three main products, because they appear faster, as well as disappear faster than those three main products. Moreover, the formation of the 5, 8 and 19-minute peaks can probably be disregarded as sequential first-order reactions for intermediates.

III. *3', 3'-cGAMP and 2', 3'-cGAMP Comparative Analysis*

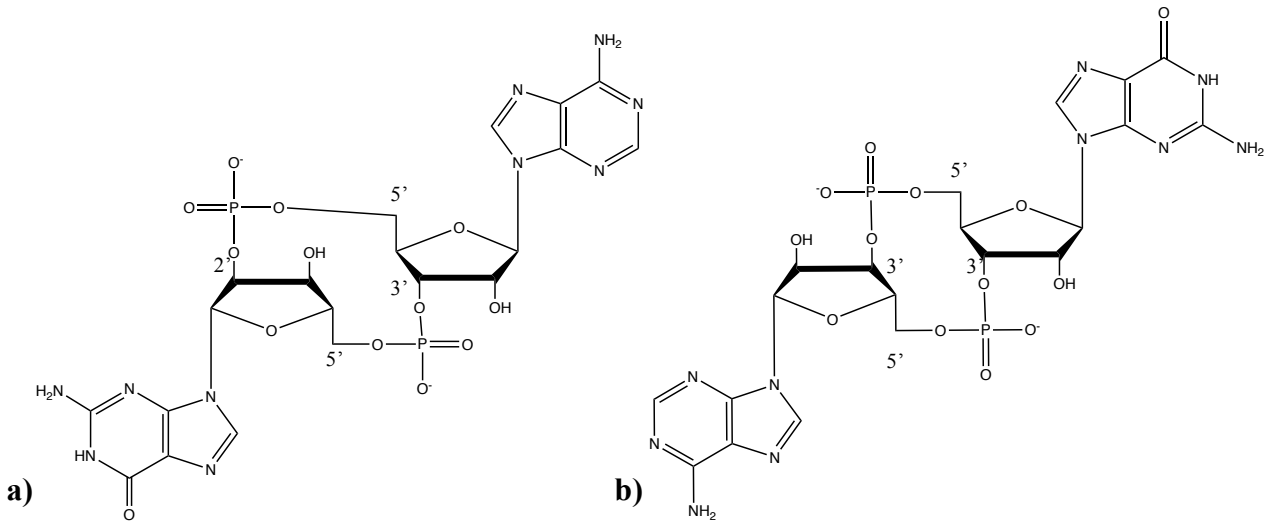

Figure 20: Molecular structure of di-cyclic nucleotide models. Figure 20a shows the molecular structure of 2', 3'-cGAMP and Figure 20b shows the molecular structure of 3', 3'-cGAMP.

Di-cyclic nucleotide models can be used in metal-ion hydrolytic reactions to study differences in kinetic profiles. Both 2', 3'- and 3', 3'-cGAMP are secondary messenger molecules that get broken down by phosphodiesterases within living organisms. The mechanism by which they each become hydrolyzed is of interest, considering they each have a different phosphate linkage. Because the 2'-phosphate linkage (from Figure 20a) is farther away from its joining 5'-ribonucleotide, the overall hydrolytic reaction may prove to be different, specifically slower, than the 3', 3'-cGAMP model, which has a 3'-phosphate linkage that is closer to its joining 5'-ribonucleotide.

After performing the same time-course for the hydrolysis reaction of 2', 3'-cGAMP as the hydrolysis reaction of 3', 3'-cGAMP, we notice that the 2', 3'-cGAMP hydrolyzes to its main products, similar to 3', 3'-cGAMP. The fact that 2', 3'-cGAMP has a different retention time on the HPLC than 3', 3'-cGAMP already proves both cyclic-dinucleotides, are structurally and chemically different from each other, despite only have a slight change in phosphodiester linkage (see Figure 20). Performing these 2', 3'-cGAMP reactions using various Ca^{2+} concentrations will allow one to see if any other intermediate peaks appear on the HPLC chromatographs, and eventually determine if a difference in catalytic efficiency exists. The fact that intermediates can be seen, at the same time-point, on some of the HPLC chromatographs for the 2', 3'-cGAMP and Ca^{2+} reaction, while no intermediates are observed for the 3', 3'-cGAMP, suggests that the hydrolytic reaction of 2', 3'-cGAMP is kinetically faster than the hydrolytic reaction of 3', 3'-cGAMP. The fact that the rate constant for the hydrolysis of 2', 3'-cGAMP in 0.33 M Ca^{2+} is about 30 times greater than the rate constant for the hydrolysis of 3', 3'-cGAMP under the same calcium concentration conditions, further confirms that 2', 3'-cGAMP cleaves at a faster rate

than 3', 3'-cGAMP (see Figure 10). Moreover, one of the possible reasons a couple of intermediates can at least be observed on the HPLC for the hydrolysis of 2', 3'-cGAMP saturated in calcium ions, is that the initial cleavage step of 2', 3'-cGAMP, which leads to the linear intermediate, occurs at a rate that is fast enough that it is able to accumulate in the reaction. As a result, the hydrolysis of 2', 3'-cGAMP saturated in 0.33 M Ca^{2+} is able to produce significant amounts of its formed intermediates, which can be detected by the HPLC. The products formed from the hydrolysis of 2', 3'-cGAMP in 0.33 M Ca^{2+} aqueous solution seem to appear at approximately the same retention times as the products formed from the hydrolysis of 3', 3'-cGAMP under the same calcium concentration conditions. The slower rate of hydrolysis of 3', 3'-cGAMP may be explained by a constrained 2'-OH group that creates difficulty to attack the phosphorus center for an in-line displacement. Instead of having a 2'-OH group that eventually behaves as a nucleophile once deprotonated, which is what is conventionally observed in RNA models, a 3'-OH group, found in 2', 3'-cGAMP, will serve as the nucleophile once it is deprotonated. Moreover, the relatively rapid degradation of 2', 3'-cGAMPmay be related to limited flexibility between the hydroxyl and phosphate groups. While a 2'-OH group is also present in the 2', 3'-cGAMP molecule, the close proximity of the 3'-OH group to the phosphate center suggests that the 3'-OH group is in a position that makes it more favorable to attack than the 2'-OH group, which is farther from the phosphate center.

All but one of the products from the hydrolysis of 2', 3'-cGAMP seem to appear at around the same retention times as the products from the hydrolysis of 3', 3'-cGAMP. We suspect that the product that is missing should have a retention time between 8 and 9 minutes, based on the chromatograph features in Figure 9. For instance, the According to Figures 7b and 7c, three products are seen, instead of the expected four products: 3'-AMP, 2'-AMP, 3'-GMP and 2'-

GMP. A product with a retention time of approximately 8 minutes (see Figure 5) is observed, which is approximately the same retention time as one of the observed products from the hydrolysis of 3', 3'-cGAMP (see Figure 5). Because the ~8-minute peak, in a 15-minute time-point, appears to have double-hump-like feature (see Figure 9b), we suspect that two products are being produced around the same retention time of approximately 8 or 9 minutes. Considering the 3'-AMP standard has a retention time of about 9 minutes and the 5-minute peak is known to contain a guanosine base (as demonstrated from the 3', 3'-cGAMP hydrolysis reactions HPLC and UV-Vis Spectroscopy Analyses), the 8-minute peak from the 2', 3'-cGAMP hydrolysis reactions may be a mixture of adenosine- and guanosine-containing products. Similarly, the 19-minute peak, from the 2', 3'-cGAMP hydrolysis reactions, is presumed to be 2'-AMP, which was decided from HPLC analyses of the 3', 3'-cGAMP hydrolysis reactions (see Figure 4). By following along with the chromatographs from the 3', 3'-cGAMP reactions (see Figure 5), the two products that are possibly combining during the HPLC separation process are 3'-AMP and 2'-GMP. Moreover, because of poor or lack of separation between the two proposed products, only a broad, single peak is observed on the chromatograph.

Similar to 3', 3'-cGAMP, four products are also expected from the hydrolysis of 2', 3'-cGAMP. The hydrolysis of both molecules should each be 2'-AMP, 3'-AMP, 2'-GMP and 3'-GMP. Because the retention time of the reactant, 2', 3'-cGAMP, on the HPLC, is approximately the same as the retention time of the peak that shows up before the 3'-AMP peak (see Figures 9a and 7a), a fourth product cannot be observed from the Ca^{2+}-assisted hydrolysis of 2', 3'-cGAMP. Figure 9b shows 3 other products peaks, not including the 2', 3'-cGAMP and intermediate peaks. Figure 9c shows a peak at about 28.8 minutes, but further trials have to be done in order to confirm whether or not it is a product from the reaction. Eventually, good separation between the

two possible peaks with retention times of about 9 minutes (see Figure 9) would be helpful in confirming the missing fourth product from the hydrolysis of 2', 3'-cGAMP. Another experiment that can be done to confirm the identity of the missing fourth product would be to spike the reaction with either 3'-AMP or 2'-GMP. Absorbance data can be gathered as well, in order to identify which products contain the guanosine and adenosine bases. After performing several trials, the observed rate constant, for the hydrolysis of 2', 3'-cGAMP, can then be calculated. Whether the reaction occurs via a di-nuclear or a mono-nuclear mechanism can also be determined from doing the kinetic studies. Differences in activation energy values and rate enhancement values can also be studied and compared between the two cyclic di-nucleotide models presented used and discussed in this research project.

References

Bellini, D; Caly D. L; McCarthy, Y; Bumann, M; An, S; Dow, M; Ryan, R. P; Walsh, M. A. "Crystal structure of an HD-GYP domain cyclic-di-GMP phosphodiesterase reveals an enzyme with a novel trinuclear catalytic iron centre." *Mol. Microbiol*. **2014**, 91, 26-28.

Bellini, D; Horrell, S; Hutchini, A; Phippen, C. W; Strange R. W; Cai, Y; Wagner, A; Webb, J. S; Tews, I; Walsh, M. A. "Dimerisation induced formation of the active site and the identification of three metal sites in EAL-phosphodiesterases." *Sci. Rep.* **2017**, 7, 1-11.

Bruice, T. C; Tsubouchi, A; Dempcy, R. O; Olson, L. P. "One- and two-metal ion catalysis of the hydrolysis of adenosine 3'-alkyl phosphate esters. Models for one- and two-metal catalysis of RNA hydrolysis." *J. Am. Chem. Soc.* **1996**, 118, 9867-9875.

Cassano, A. G; Anderson, V. E; Harris, M. E. "Analysis of solvent nucleophile isotope effects: evidence for concerted mechanisms and nucleophilic activation by metal coordination in nonenzymatic and ribozyme-catalyzed phosphodiester hydrolysis." *Biochemistry*. **2004**, 43, 10547-10559.

Cassano, A. G; Anderson, V. E; Harris, M. E. "Understanding the transition states of phosphodiester bond cleavage: Insights from heavy atom isotope effects." *Biopolymers*. **2004**, 73, 110-129.

Chval, Z; Chvalová, D; Leclerc, F. "Modeling the RNA 2'OH activation: possible roles of metal ion and nucleobase as catalysts in self-cleaving ribozymes." *J. Phys. Chem.* **2011**, 115, 10943-10956.

Fischer, J. H. "Specific detection of nucleotides, creatine phosphate, and their derivatives from tissue samples in a simple, isocratic, recycling, low-volume system." *LC-GC International*. **1995**, 8, 254-264.

Gao, J; Tao, J; Liang, W; Zhao, M; Du, X; Cui, S; Duan, H; Kan, B; Su, X; Jiang, Z. "Identification and characterization of phosphodiesterases that specifically degrade 3'3'-cyclic GMP-AMP." *Cell Res*. **2015**, 25, 539-550.

Hallberg, Z. F; Wang, X. C; Wright, T. A; Nan, B; Ad, O; Yeo, J; Hammond, M. C. "Hybrid promiscuous (Hypr) GGDEF enzymes produce cyclic AMP-GMP (3', 3'-cGAMP)." *PNAS*. **2016**, 113, 1790-1795.

Hegg, E. L; Deal, K. A; Kiessling, L. L; Burstyn, J. N. "Hydrolysis of double-stranded and single-stranded RNA in hairpin structures by the copper(II) macrocyle Cu([9]aneN3)Cl2." *Inorg. Chem.* **1997**, 36, 1715-1718.

Hengge, Alvan C (January 2015) Phosphoryl Transfer Reactions. In: eLS. John Wiley & Sons, Ltd: Chichester. DOI: 10.1002/9780470015902.a0000608.pub2

Kalia, D; Merey, G; Nakayama, S; Zheng, Y; Zhou, J; Luo, Y; Guo, M; Roembke, B. T; Sintim, H. O. "Nucleotide, c-di-GMP, c-di-AMP, cGMP, cAMP, (p)ppGpp signaling in bacteria and implications in pathogenesis." *Chem. Soc. Rev.* **2013**, 42, 305-341.

Kato, K; Nishimasu, H; Oikawa, D; Hirano, S; Hirano, H; Kasuya, G; Ishitani, R, Tokunaga, F; Nureki, O. "Structural insights into cGAMP degradation by Ecto-nucleotide pyrophosphatase phosphodiesterase 1." *Nat. Commun*. **2018**, 9, 4424. DOI: 10.1038/s41467-018-06922-7.

Kirk, B. A; Cusack, C. L; Laager, E; Rochlis, E; Thomas, T; Cassano, A. G. "Mononuclear and dinuclear mechanisms for catalysis of phosphodiester cleavage by alkaline earth metal ions in aqueous solution." *J. Inorg. Biochem*. **2010**, 104, 2017-210.

Komiyama, M; Sumaoka, J. "Progress towards synthetic enzymes for phosphoester hydrolysis." *Curr. Opin. Chem. Biol.* **1998**, 2, 751-757.

Korhonen, H; Koivusalo, T; Toivola, S; Mikkola, S. "There is no universal mechanism for the cleavage of RNA model compounds in the presence of metal ion catalysts." *Org. Biomol. Chem.* **2013**, 11, 8324-8339.

Král, V; Lang, K; Králová; Dvorák; Martásek; Chin A. O; Andrievsky, A; Lynch V; Sessler J. L. "Polyhydroxylated sapphyrins: multisite non-metallic catalysts for activated phosphodiester hydrolysis." *J. Am. Chem. Soc.* **2006**, 128, 432-437.

Kranzusch, P. J; Lee, A. S. Y; Wilson, S. C; Solovykh; Vance, R. E; Berger, J. M; Doudna, J. A. "Structure-guided reprogramming of human cGAS dinucleotide linkage specificity." *Cell*. **2014**, 158, 1011-1021.

Lassila, J. K; Zalatan, J. G; Herschlag, D. "Biological phosphoryl-transfer reactions: Understanding mechanism and catalysis." *Annu. Rev. Biochem.* **2011**, 80, 669-702.

Li, Y; Breaker, R. R. "Kinetics of RNA degradation by specific base catalysis of transesterification involving the 2'-hydroxyl group." *J. Am. Chem. Soc.* **1999**, 121, 5364-5372.

Lönnberg, H. "Cleavage of RNA phosphodiester bonds by small molecular entities: a mechanistic insight." *Org. Biomol. Chem.* **2011**, 9, 1687-1703.

Messina, K. Investigation of the Mechanism of Ca^{2+} Catalyzed RNA Phosphodiester Hydrolysis. BA with Specialized Honors in Chemistry, Drew University, May 2014.

Mikkola, S; Stenman, E; Nurmi, K; Yousefi, E; Strömberg, R; Lönnberg, H. "The mechanism of the metal ion promoted cleavage of RNA phosphodiester bonds involved a general acid catalysis by the metal aquo ion on the departure of the leaving group." *J. Chem. Soc., Perkin Trans. 2*. **1999**, 1619-1625.

Minasov, G; Padavattan, S; Shuvalova, L; Brunzelle, J. S; Miller, D. J; Baslé, A; Massa, C; Collart, F. R; Schirmer, T; Anderson, W. F. "Crystal structures of Ykul and its complex with second messenger cyclic di-GMP suggest catalytic mechanism of phosphodiester bond cleavage by EAL domains." *J. Biol. Chem.* **2009**, 284, 13174-13184.

Namasivayam, V; Lee, S; Müller, C. E. "The promiscuous ectonucleotidase NPP1: molecular insights into substrate binding and hydrolysis." *Biochimica et Biophysica Acta.* **2017**, 1861, 603-614.

Ora, M; Martikainen, K; Lautkoski, K. "Hydrolytic reactions of cyclic bis(3'-5') diadenylic acid (c-di-AMP)." *J. Phys. Org. Chem*. **2013**, 26, 218-225.

Oivanen, M; Kuusela, S; Lönnberg H. "Kinetics and mechanisms for the cleavage and isomerization of the phosphodiester bonds of RNA by BrØnsted acids and bases." *Chem. Rev.* **1998**, 98, 961-990.

Oivanen, M; Schnell, R; Pfleiferer, W; Lönnberg, H. "Interconversion and hydrolysis of monomethyl and monoisopropyl esters of adenosine 2'- and 3'-monophosphates: kinetics and mechanisms." *J. Org. Chem.* **1991**, 56, 3623-3628.

Rao, F; Yang, Y; Yaning, Q; Liang, Z. "Catalytic mechanism of cyclic di-GMP-specific phosphodiesterase: a study of the EAL domain-containing RocR from *Pseudomonas aeruginosa*." *J. Bacteriol*. **2008**, 190, 3622-3631.

Robinson H; Jung, K; Switzer, C; Wang, A. H. "DNA with 2'-5' phosphodiester bonds forms a duplex structure in the A-type conformation." *J. Am. Chem. Soc.* **1995**, 117, 837-838.

Römling, U; Liang, Z; Dow, M. "Progress in understanding the molecular basis underlying functional diversification of cyclic dinucleotide turnover proteins." J. Bacteriol. 2017, 199

Schmidt, A. J; Ryjenkov, D. A; Gomelsky, M. "The ubiquitous protein domain EAL is a cyclic diguanylate-specific phosphodiesterase: enzymatically active and inactive EAL domains." *J. Bacteriol.* **2005**, 187, 4774-4781.

Shanahan, C. A; Gaffney, B. L; Jones, R. A; Strobel, S. A. "Identification of c-di-GMP derivatives resistant to an EAL domain phosphodiesterase." *Biochemistry*. **2013**, 52, 365-377.

Smith, K. D; Lipchock S. V; Strobel S. A. "Structural and biochemical characterization of linear dinucleotide analogues bound to the c-di-GMP-I aptamer." *Biochemistry*. **2012**, 51, 425-432.

Tchigvintsev, A; Xu, X; Singer, A; Chang, C; Brown, G; Proudfoot, M; Cui, H; Flick, R; Anderson, W. F; Joachimiak, A; Galperin, M. Y; Savchenko, A; Yakunin, A. F. "Structural

insight into the mechanism of c-di-GMP hydrolysis by EAL domain phosphodiesterases." *J. Mol. Bio*. **2010**, 402, 524-538.

Torres, R. A; Himo, F; Bruice, T.C; Noodleman, L; Lovell, T. "Theoretical examination of Mg^{2+}-mediated hydrolysis of a phosphodiester linkage as proposed for the Hammerhead ribozyme." *J. Am. Chem. Soc.* **2003**, 125, 9861-98667.

Yashiro, M; Higuchi, M; Washizu, Y; Komiyama, M. "Effect of alkaline earth metal ions on the phosphodiester hydrolysis of RNA." *Bull. Chem. Soc. Jpn*. **2002**, 75, 1843-1844.

Verma, S; Mishra, A. K; Kumar, J. "Many facets of adenine: coordination, crystal patterns, and catalysis." *Acc. Chem. Res.* **2010**, 43, 79-91.

Westheimer, F. H. "Why nature chose phosphates." *Science*. **1987**, 235, 1173-1178.

Wu, J; Sun, L; Chen, X; Du, F; Shi, H; Chen C; Chen, Z. J. "Cyclic-GMP-AMP is an endogenous second messenger in innate immune signaling by cytosolic DNA." *Science*. **2013**, 339, 826-830.

Zhan, C; Zheng, F. "First computational evidence for a catalytic bridging hydroxide ion in a phosphodiesterase active site." *J. Am. Chem. Soc.* **2001**, 123, 2835-2838.

Zagórowska, I; Kuusela, S; Lönnberg, H. "Metal ion-dependent hydrolysis of RNA phosphodiester bonds with hairpin loops. A comparative kinetic study on chimeric ribo/2'-*O*-methylribo oligonucleotides." *Nucleic Acids Res.* **1998**, 26, 3392-3396.